Data Collection Path Planning with Spatially Correlated Measurements using Growing Self-Organizing Array

Jan Faigl

Department of Computer Science, Faculty of Electrical Engineering, Czech Technical University in Prague, Technická 2, 166 27, Prague 6, Czech Republic

Abstract

Data collection path planning is a problem to determine a cost-efficient path to read the most valuable data from a given set of sensors. The problem can be formulated as a variant of the combinatorial optimization problems that are called the price-collecting traveling salesman problem or the orienteering problem in a case of the explicitly limited travel budget. In these problems, each location is associated with a reward characterizing the importance of the data from the particular sensor location. The used simplifying assumption is to consider the measurements at particular locations independent, which may be valid, e.g., for very distant locations. However, measurements taken from spatially close locations can be correlated, and data collected from one location may also include information about the nearby locations. Then, the particular importance of the data depends on the currently selected sensors to be visited by the data collection path, and the travel cost can be saved by avoiding visitation of the locations that do not provide added value to the collected data. This is a computationally challenging problem because of mutual dependency on the cost of data collection path and the possibly collected rewards along such a path. A novel solution based on unsupervised learning method called the Growing Self-Organizing Array (GSOA) is proposed to address computational challenges of these problems and provide a solution in tens of milliseconds using conventional computational resources. Moreover, the employed GSOA-based approach allows to exploit capability to retrieve data by wireless communication or remote sensing, and thus further save the travel cost.

Keywords: Unsupervised learning, Data-Collection Planning, Spatial Correlations, GSOA

1. Introduction

Autonomous data collection is a problem studied in robotics in which one or several robotic vehicles are requested to collect the most valuable sensor measurements from a given set of sensors in a cost-efficient way or even with an explicitly limited travel budget. The problem is motivated by several practical scenarios such as data retrieving from pre-deployed sensor networks [1] to study ocean floor [2, 3], monitoring algae blooms [4], volcanic activity [5, 6], and pollution monitoring [7] or environment monitoring missions [8]. The problem is to determine a cost-efficient path to visit a set of sensor locations that can be formulated as the combinatorial *Traveling Salesman Problem* (TSP) [9], which is known to be NP-hard unless P=NP [10].

Data from a sensor can be remotely retrieved using wireless communication [11], and thus a precise visitation of the sensor locations can be avoided to save the travel cost. Such an extension of the TSP is called the *TSP with Neighborhoods* (TSPN) or with explicitly specified disk-shaped neighborhoods for a symmetric communication range δ as the *Close Enough TSP* (CETSP) [12], e.g., used in forest fire detection in [13]. Since for $\delta = 0$ the problem becomes the TSP, also the TSPN is NP-hard.

Solving the TSPN (or CETSP) optimally is computationally very demanding, e.g., using Mixed Integer Non-linear Programming [14], and thus heuristic approaches [15, 16] and evolutionary techniques have been proposed [17] including unsupervised learning approaches [18, 19]. Besides, the CETSP can be addressed by an explicit sampling of the possible locations within the particular disk-shaped neighborhood around each sensor location, and the problem can be solved as the *Generalized TSP* (GTSP) [20] using heuristic approaches [21, 22]. The main drawback of this sampling-based approach is that the size of the problem is quickly increasing for a simple sampling strategy and a solution of such a transformed problem is computationally demanding [23].

In addition to the challenges related to the remote sensing or data retrieving within the δ range [24], another important part of data collection planning is the fact that the quality of data retrieved from each sensor can be characterized as expected information received. Therefore, it may be suitable to avoid visitation of sensors that provide less important data in a benefit of reducing the travel cost or collecting more rewarding data from a distant location. This aspect can be considered in formulation of the data collection planning as the *Prize-Collecting TSP* (PCTSP) [25], i.e., extended to the *PCTSP with Neighborhoods* (PCTSPN) [26], or the *Orienteering Problem* (OP) [27, 28] that has been relatively recently generalized into the *OP with Neighborhoods* (OPN) [29, 30, 31].

In the PCTSP, each sensor has associated a penalty if data from the sensor are not collected and the problem is to determine a path such that the sum of the path length and sum of the penalties for not visiting sensors is minimal. For the OP, each sensor has associated reward for the retrieved data from it, but the main difference is that the length of the data collection path maximizing the sum of the collected rewards has not to exceed the given travel budget $\mathrm{T}_{\max}$ [27].

Both the PCTSPN and OPN formulations can be utilized for planning a data collection path to retrieve data from the most rewarding sensors; however, in most of the existing approaches (further described in Section 2), the measurements are considered independent, and thus also the rewards associated to the sensors are fixed, i.e., the reward (penalty) value of the particular sensor does not depend on the collected data from other sensors. Although such an assumption may hold for many practical cases, there are also problems where the collected data are used for modeling and predicting large-scale and spatially correlated environment phenomena [32]. In such a case, the solution becomes more challenging as the reward values depend on the currently selected sensors to be visited by the data collection path.

In this paper, the data collection planning with spatially correlated measurements is addressed. The proposed solution originates from the previous successful deployment of unsupervised learning methods in the solution of the PCTSPN [33], OPN [31], and early results on the PCTSPN with spatial correlations reported in [34]. However, a novel unsupervised learning procedure for routing problems called the *Growing Self-Organizing Array* (GSOA) [19] is employed in the presented approach to solving the close enough variants of the PCTSP and OP with spatially correlated measurements. Since the presented work originates in the previous approaches, the particular contributions are considered as follows:

- Generalization of the GSOA for the CETSP [19] to the solution of the Close Enough PCTSP (CEPCTSP)
- and its further extension to the problems with spatially correlated measurements.
- Novel GSOA-based solution of the Close Enough Orienteering Problem (CEOP)
- with comparison to the previous unsupervised learning based approaches;
- and its application to problems with spatially correlated measurements.

Beside of that, the herein proposed approach is the first deployment of the GSOA [19] in the solution of the orienteering problems. Specifically, the proposed GSOA-based solver provides competitive solutions to the previous unsupervised learning based approaches to the OP, it improves the solution quality in the CEOP, and it is also capable to exploit spatial correlation of the measurements. Thus, the presented GSOA approach provides solution of the whole class of the data collection planning problems including CETSP, CEPCTSP, OP, and CEOP all with spatially correlated measurements.

The remainder of the paper is organized as follows. An overview of the related work on the PCTSP, OP, and also correlated measurements is presented in the following section. Formulations of the addressed problems together with the model of the spatial correlations are in Section 3. The proposed GSOA-based solutions of the Close Enough PCTSP and OP are presented in Section 4 and results on their evaluations and comparisons with existing approaches are reported in Section 5. Finally, Section 6 is dedicated to the concluding remarks.

2. Related Work

Two main problem formulations can be found in the literature to solve data collection path planning, the Prize-Collecting TSP (PCTSP) [25] and the Orienteering Problem (OP) [27]. Both problem formulations can be extended to their variants with the neighborhoods and also spatial correlations. An overview of the existing approaches is presented in this section to provide a context and emphasize the main challenges.

Existing approaches for the PCTSP include approximate algorithms [35, 36] and unsupervised learning technique [37]. The PCTSPN extends the problem to determine the particular locations where the data are retrieved from the sensors, which allows exploiting retrieving data remotely from the sensors. Authors of [26] address the PCTSPN by a decoupled approach that combines heuristics to determine locations inside the respective neighborhood of the sensors and a solution of the standard TSP to find the path connecting the locations. A unifying approach based on unsupervised learning has been presented in [33] which directly addresses the continuous space of the neighborhood of each sensor. Despite the approach [33] does not utilize the explicit sampling of the neighborhood into a pre-specified discrete set as [26], it is less computationally demanding, and it provides significantly better solutions.

Even though the PCTSPN can be used for planning data collection paths, the main drawback of this formulation is the question how to balance the trade-off between the path length and the sum of penalties for not visited sensors. There is a single objective function in the PCTSP formulation in which the total solution cost is the sum of the travel cost (the path length) and the penalties for not visited sensors, e.g., see Problem 3.1. If the balance is not easy to setup, it may be more suitable to formulate the data collection planning problem as the OP or as the OPN to exploit a non-zero communication range δ.

Many approaches and variants of the OP have been proposed in the literature [38, 28]. On the other hand, an explicit solution of the OPN has been introduced relatively recently and the first such a solution is based on the unsupervised learning techniques [29, 30, 31, 39]. Besides, the Variable Neighborhood Search (VNS) metaheuristic [40] can be utilized for sampled neighborhoods into discrete sets, but such a solution is computationally very demanding.

Probably the first approach directly addressing the spatially correlated measurements in data collection planning has been proposed in [41]. The authors formulate the data collection planning problem on a discrete graph, where rewards are associated with the nodes of the graph and the rewards may be related to the neighborhood nodes.

The problem is called the *Correlated Orienteering Problem* (COP), and the proposed solution is based on Mixed Integer Quadratic Programming (MIQP). The reported results are for graphs formed as a grid with up to 12×12 nodes for which solutions are found in tens or hundreds of seconds using Intel Core-i7 5820 CPU [41].

Another recent approach addressing the data collection planning with spatially correlated measurements is based on unsupervised learning technique previously employed in the solution of the PCTSPN [34]. The authors exploit low computationally requirements of [33] and update the reward values during the learning. The influence of visiting one location to the rewards (penalties) of the neighboring locations are considered in a continuous space, contrary to the discrete model of [41]. The rewards (penalties) are updated based on the idea that measurements from one or several locations may also include information about the measurements at the nearby locations.

In [34], it is assumed that the influence of spatial correlations is decreasing with the distance of the sensor locations and from a specific distance, the measurements are not correlated at all. The spatial correlation is therefore formulated as a distance based model of correlation between the sensor measurements. The actual value of the reward is determined online from the default value of the reward r (without the influence of the other sensors) proportionally decreased by the ratio computed from the geometrical relations of the neighboring sensors using the so-called correlation radius χ and reward (penalty) radius ξ of the involved sensors.

Performance of the method proposed in [34] is demonstrated in the same PCTSPN scenario as in [33], further denoted as the OOI, and the reported computational requirements are in tens of milliseconds using similar computational resources as in [41] but with utilizing only a single core of the CPU. The solution cost is a bit improved if spatial correlations are considered in comparison to the previous approach [33]; however, with increasing communication range δ, such a benefit is less noticeable.

The MIQP-based approach [41] is formulated on a discrete graph where the travel cost from one location to another location is a weight of the particular edge. On the other hand, the unsupervised learning method [34] is considered in the continuous space which provides an advantage of determining suitable locations for collecting the rewards during the solution of the problem; and the travel cost is directly computed as the Euclidean distance between two respective locations. However, the unsupervised learning can be deployed on a graph [42] and the Euclidean distance can be replaced by point-to-point path planning using a motion planning roadmap [43] at the cost of more complex and more demanding algorithm. Besides, an artificial potential field has been used as a navigation function in [44], and therefore, similar approaches such as [45] can be eventually utilized.

Here, it is worth mentioning that the learning techniques employed in [33] and [31] have been consolidated and conceptually simplified into unifying unsupervised learning based approach for solving routing problems in [19]. The novel method is called the *Growing Self-Organizing Array* (GSOA). Even though the GSOA originates from the SOM-based approaches for the TSP, one of its main advantages is that it directly supports the selection of the most rewarding sensors in the data collection planning problems with an adjustment of the number of learning nodes, contrary to SOM-based approaches that require a fixed number of neurons defined prior the learning, e.g., see [46, 47, 48]. Besides, it does not need explicit parameter tuning.

In [19], the GSOA is evaluated and compared with other state-of-the-art SOM-based solvers for the regular TSP in representative benchmarks of the TSPLIB [49], where it provides the best trade-off between the solution quality and the required computational time. Moreover, the GSOA has also been evaluated and compared in the solution of the CETSP instances where it provides competitive or better results than the heuristic approaches, but it is about three orders of magnitude faster than a heuristic based on a solution of the related GTSP [19]. Another advantage of the GSOA is its flexibility to solve CETSP instances with individual communication radius per each sensor, and thus it supports local properties of the sensors surroundings and communication capabilities of each sensor.

Based on the overview of the existing approaches and results reported therein, the GSOA is considered as the promising approach to address data collection planning with spatially correlated measurements in a new unifying way. Further, motivated by the evaluation presented in [19], the PCTSPN and OPN are rather called the *Close Enough PCTSP* (CEPCTSP) and *Close Enough OP* (CEOP) to emphasize the disk-shaped neighborhoods of the sensors. Therefore, the GSOA is applied in the solution of the CEPCTSP and CEOP with spatially correlated measurements using the geometrical model of the spatial correlations proposed in [34]. The particular formulations of the problems addressed in this paper are presented in the following section.

3. Problem Statement and Formulations

The data collection planning addressed in this paper is formulated as two problems that can be found in the literature, the Prize-Collecting Traveling Salesman Problem (PCTSP) and Orienteering Problem (OP) both considered in their close enough variants to exploit capability to retrieve data from the sensors within the communication range δ, and thus save the travel cost. Besides, both problems are considered with spatially correlated measurements that may influence the associated rewards (penalties) to the sensors if data from the nearby sensors are retrieved along the data collection path being found. The problems are formally introduced in the following paragraphs, but the model of spatial correlation is addressed separately (in Section 3.1) to make the problem definitions clear and readable as it only changes the way how the rewards are computed.

Both the problem formulations share the description of the data collection mission that consists of the set of n sensors $\mathbf{S}$ located in a plane, $\mathbf{S} \subset \mathbb{R}^2$. The position of each sensor s_i is known and for simplicity and with a slightly overloaded notation, the sensor location is denoted $\boldsymbol{s}_i$ and $\mathbf{S} = \{\boldsymbol{s}_1, \ldots, \boldsymbol{s}_n\}$, i.e., $\boldsymbol{s}_i \in \mathbb{R}^2$. The data collection vehicles are operating in $\mathbb{R}^2$ with a constant average velocity. The travel cost $c(\boldsymbol{p}_1, \boldsymbol{p}_2)$ between $\boldsymbol{p}_1 \in \mathbb{R}^2$ and $\boldsymbol{p}_2 \in \mathbb{R}^2$ can be directly computed from the Euclidean distance between $\boldsymbol{p}_1$ and $\boldsymbol{p}_2$ and it is assumed w.l.o.g. $c(\boldsymbol{p}_1, \boldsymbol{p}_2) = \|(\boldsymbol{p}_1, \boldsymbol{p}_2)\|$.

In the original formulation of the PCTSP [25], it is considered that each sensor s_i has associated penalty $\zeta(s_i) \geq 0$, while rewards $r(s_i) \geq 0$ are considered in the OP [27]. The herein presented formulation of the PCTSP is slightly modified to unify the symbols and notation of the PCTSP and the OP. The penalties $\zeta(s_i)$ are considered as the rewards $r(s_i)$, but since the sum of penalties is combined with the travel cost in the PCTSP, it is necessary to scale the reward value to the penalty and $\zeta(s_i) = \lambda r(s_i)$ and w.l.o.g., $\lambda = 1$ is considered to simplify the notation. In the rest of the paper, r_i is used instead of $r(s_i)$ whenever it is clear the reward is associated with the i-th sensor s_i.

In planning a data collection path, we are searching for a subset of k sensors $\mathbf{S}_k \subseteq \mathbf{S}$ from which the most rewarding data are collected along the cost-efficient path. Therefore, the data collection path can be specified by a permutation Σ_k defining the order of visits to the sensors $\mathbf{S}_k$, and Σ_k is a permutation of the sensor labels $\Sigma_k = (\sigma_1, \ldots, \sigma_k)$, where $1 \leq \sigma_i \leq n$ and $\sigma_i \neq \sigma_j$ for $i \neq j$.

Having these preliminaries and not considering the communication range, i.e., $\delta = 0$, the PCTSP can be formulated as Problem 3.1. W.l.o.g. the vehicle starting location is considered to be the sensor location $\mathbf{s}_1$, i.e., $\sigma_1 = 1$, and it is always selected to be in $\mathbf{S}_k$.

Problem 3.1 (PCTSP – Prize-Collecting TSP).

$$\min_{1\le k\le n, \mathbf{S}_k\subseteq\mathbf{S}, \Sigma_k} \quad C(\mathbf{S}_k, \Sigma_k) \tag{1}$$

$$C(\mathbf{S}_k, \Sigma_k) \quad = \quad \sum_{i=1}^{k-1} \left\|(\boldsymbol{s}_{\sigma_i}, \boldsymbol{s}_{\sigma_{i+1}})\right\| \tag{2}$$

$$+ \left\|(\boldsymbol{s}_{\sigma_k}, \boldsymbol{s}_{\sigma_1})\right\| \tag{3}$$

$$\lambda \sum_{s_j\in\mathbf{S}\setminus\mathbf{S}_k} r(s_j) \tag{4}$$

$$\text{s.t.} \qquad 1\le k\le n; \quad 1\le \sigma_i\le n; \quad \sigma_i\in\Sigma_k$$

$$\boldsymbol{s}_{\sigma_i}\in\mathbf{S_k}; \quad \boldsymbol{s}_{\sigma_1}=\boldsymbol{s}_1; \quad s_1\in\mathbf{S}_k$$

The term (3) is because the PCTSP follows the TSP where the requested path has to be closed, and the term (4) represents the sum of penalties for not visited sensors.

For the Close Enough PCTSP (CEPCTSP), it is allowed to retrieve data from s_i within the range δ_i. Therefore, the problem is not only to determine the subset $\mathbf{S}_k$ of k sensors and the order of visits Σ_k to minimize the cost function $C(\mathbf{S}_k, \Sigma_k)$, but also the most suitable waypoint locations $\mathbf{P}=\{\boldsymbol{p}_{\sigma_1},\ldots,\boldsymbol{p}_{\sigma_k}\}$, $\boldsymbol{p}_i\in\mathbb{R}^2$ are requested to be found such that $\|(\boldsymbol{p}_i, \boldsymbol{s}_i)\|\le\delta_i$. Hence, the CEPCTSP is not a purely combinatorial problem as the PCTSP, and it includes a continuous optimization part as the particular waypoint can be arbitrarily selected within the distance δ_i from the respective sensor location $\boldsymbol{s}_i$.

Problem 3.2 (CEPCTSP – Close Enough PCTSP).

$$\min_{1\le k\le n, \mathbf{S}_k\subseteq\mathbf{S}, \Sigma_k, \mathbf{P}_k\subset\mathbb{R}^2} \quad C(\mathbf{S}_k, \Sigma_k, \mathbf{P}_k) \tag{5}$$

$$C(\mathbf{S}_k, \Sigma_k, \mathbf{P}_k) \quad = \quad \sum_{i=1}^{k-1} \left\|(\boldsymbol{p}_{\sigma_i}, \boldsymbol{p}_{\sigma_{i+1}})\right\| \tag{6}$$

$$+ \left\|(\boldsymbol{p}_{\sigma_k}, \boldsymbol{p}_{\sigma_1})\right\| \tag{7}$$

$$\lambda \sum_{s_j\in\mathbf{S}\setminus\mathbf{S}_k} r(s_j)$$

$$\text{s.t.} \qquad 1\le k\le n; \quad 1\le \sigma_i\le n; \quad \sigma_i\in\Sigma_k$$

$$\boldsymbol{s}_{\sigma_i}\in\mathbf{S_k}; \quad \boldsymbol{s}_{\sigma_1}=\boldsymbol{s}_1; \quad s_1\in\mathbf{S}_k$$

$$\boldsymbol{p}_{\sigma_i}\in\mathbf{P_k}; \quad \left\|(\boldsymbol{p}_{\sigma_i}, \boldsymbol{s}_{\sigma_i})\right\|\le\delta_i$$

Notice, we assume the initial location of the vehicle is s_1, and therefore, it may be suitable to set $\delta_1=0$. The communication radius can be individual per each sensor; however, a single δ is used in the rest of the paper whenever the radii are considered the same to simplify the notation.

The OP is similar to the PCTSP in selecting the most rewarding sensors, but it differs in explicitly prescribed travel budget and maximizing the total collected rewards. Besides, the original formulation [27] specifies the initial and final locations of the data collection vehicle which are w.l.o.g. defined as s_1 and s_n, both with the zero rewards

$r_1 = r_n = 0$. The OP is combinatorial optimization problem to select k sensors $\mathbf{S}_k \subseteq \mathbf{S}$ with the maximal sum of the rewards such that the length of the path connecting them (that starts at s_1 and terminates at s_n) does not exceed the travel budget $\mathrm{T}_{\max}$. Thus, at least two sensors are selected[1] in $\mathbf{S}_k$, i.e., $k \geq 2$ and $\sigma_1 = 1$ and $\sigma_k = n$. The OP is formally defined as Problem 3.3.

Problem 3.3 (OP – Orienteering Problem).

$$\max_{k,\mathbf{S}_k\subseteq\mathbf{S},\Sigma_k} \quad R(\mathbf{S}_k, \Sigma_k) = \sum_{i=1}^{k} r(s_{\sigma_i}) \tag{8}$$

$$\begin{aligned} \text{s.t.} \quad & \sum_{i=1}^{k-1} \left\|(\boldsymbol{s}_{\sigma_i}, \boldsymbol{s}_{\sigma_{i+1}})\right\| \leq \mathrm{T}_{\max} \\ & \Sigma_k = (\sigma_1, \ldots, \sigma_k); \quad 2 \leq k \leq n \\ & 1 \leq \sigma_i \leq n; \quad \sigma_1 = 1; \quad \sigma_k = n \\ & \boldsymbol{s}_{\sigma_i} \in \mathbf{S}_k; \quad \boldsymbol{s}_{\sigma_1} = \boldsymbol{s}_1, \ \boldsymbol{s}_{\sigma_k} = \boldsymbol{s}_n \end{aligned} \tag{9}$$

Similarly to the CEPCTSP, the waypoints $\mathbf{P}_k$ at which data from the selected sensors are retrieved are determined in the Close Enough OP (CEOP), where we consider $\delta_1 = \delta_n = 0$ as it is requested to start and finish the mission exactly at the locations s_1 and s_n, respectively, and thus $\boldsymbol{p}_1 = \boldsymbol{s}_1$ and $\boldsymbol{p}_k = \boldsymbol{s}_n$. The CEOP is formally defined as Problem 3.4.

Problem 3.4 (CEOP – Close Enough OP).

$$\max_{k,\mathbf{S}_k\subseteq\mathbf{S},\Sigma_k,\mathbf{P}_k} R(\mathbf{S}_k, \Sigma_k, \mathbf{P}_k) = \sum_{i=1}^{k} r(s_{\sigma_i}) \tag{10}$$

$$\begin{aligned} s.t. \quad & \sum_{i=1}^{k-1} \left\|(\boldsymbol{p}_{\sigma_i}, \boldsymbol{p}_{\sigma_{i+1}})\right\| \leq \mathrm{T}_{\max} \\ & \Sigma_k = (\sigma_1, \ldots, \sigma_k); \quad 2 \leq k \leq n \\ & 1 \leq \sigma_i \leq n; \quad \sigma_1 = 1; \quad \sigma_k = n \\ & \boldsymbol{s}_{\sigma_i} \in \mathbf{S}_k; \quad \boldsymbol{s}_{\sigma_1} = \boldsymbol{s}_1, \ \boldsymbol{s}_{\sigma_k} = \boldsymbol{s}_n \\ & \left\|(\boldsymbol{p}_{\sigma_i}, \boldsymbol{s}_{\sigma_i})\right\| \leq \delta_{\sigma_i}; \quad \boldsymbol{p}_1 = \boldsymbol{s}_1; \quad \boldsymbol{p}_k = \boldsymbol{s}_n \end{aligned} \tag{11}$$

3.1. Model of Spatially Correlated Sensor Measurements

A distance-based model of the spatially correlated measurements has been presented in [30]; however, it is briefly described here to make the paper self-contained. The main idea of the model is that the value of the reward (penalty) characterizing the possible information gain of the collected data from a particular sensor s_i depends on how much data from the nearby sensors are collected. Thus, including a particular sensor in the selected subset $\mathbf{S}_k$ may decrease rewards of the nearby sensors from $\mathbf{S} \setminus \mathbf{S}_k$.

In general, data are collected to study some spatial or even spatiotemporal phenomena that can be modeled as a time-varying scalar field, $\Psi(\boldsymbol{p}, t)$, $\boldsymbol{p} \in \mathbb{R}^2$ [41]. Having the sampled data at the sensor locations $\mathbf{S}$, the problem is to create a model of the field from the collected values $\Psi(\boldsymbol{s}_i, t)$ at the particular sensor locations $\boldsymbol{s}_i \in \mathbf{S}$. In [41],

[1] It is assumed the travel budget $\mathrm{T}_{\max}$ is at least $\mathrm{T}_{\max} \geq \|(s_1, s_n)\|$ otherwise a feasible solution does not exist.

the authors model the spatial relations in a graph $G(V, E)$ where V denotes the sensors and $G(V, E)$ has an edge (v_i, v_j) if and only if $\Psi(v_j, t)$ is dependent on $\Psi(v_i, t)$, i.e., measurements at corresponding sensor locations $\boldsymbol{s}_j$ and $\boldsymbol{s}_i$, respectively. $\Psi(v_i, t)$ can have a form

$$\Psi(v_i, t) = f_i(\Psi(v_{i_1}, t), \ldots, \Psi(v_{i_l}, t)), \tag{12}$$

where $N_i = \{v_{i_1}, \ldots, v_{i_l}\}$ are the neighboring sensors of v_i in the graph $G(V, E)$.

Having a subset of the selected sensors $\mathbf{S}_k$ with the corresponding subset $V_k \subseteq V$, the quality of the field model created from the collected data $\Psi(v_i, t)$ for $v_i \in V_k$ can be computed as the reward function $J : \{\mathbf{S}_k\} \rightarrow \mathbb{R}^+ \cup \{0\}$ that maps data from the sensors $\mathbf{S}_k$ to real values [41]. The contribution of measurements from a sensor s_i can be then expressed as

$$J_{\mathbf{S}_k}(s_i) = J(\mathbf{S}_k \cup \{s_i\}) - J(\mathbf{S}_k). \tag{13}$$

Using (13), we can compute the default reward $r(s_i)$ considering $\mathbf{S}_k = \emptyset$. Then, during the solution of the PCTSP or OP, the reward value of the sensors not included in the currently selected $\mathbf{S}_k$ can be updated, i.e., $r(s_i) = J_{\mathbf{S}_k}(s_i)$.

Despite the fact that the formulas (12) and (13) provide a general way how to compute the rewards, its particular evaluation depends on the phenomena studied from the collected measurements. Therefore the distance-based model of the spatial correlations has been proposed in [34] to evaluate benefits of considering spatial correlations in the solution of the PCTSP in a phenomenon independent way. In this paper, we follow this model which is summarized in the rest of this section.

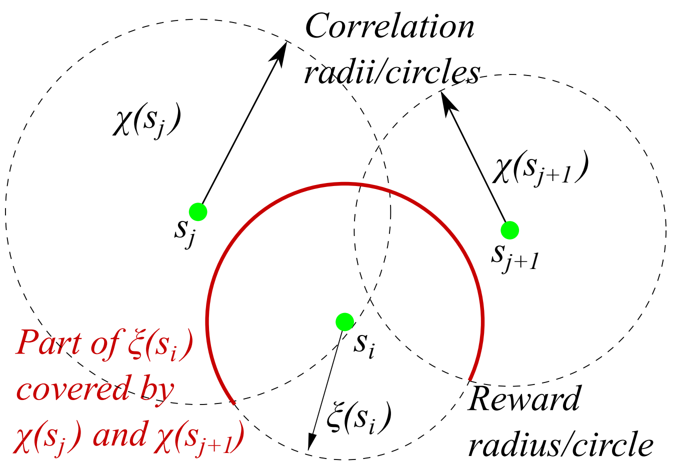

Figure 1: Geometrical relations of the correlation and penalty radii in the utilized distance-based model of the spatial correlations proposed in [34]. The default reward of the sensor s_i is decreased proportionally to the covered part (shown in red) of the circle with the reward radius $\xi(s_i)$ centered at $\mathbf{s}_i$ that is within the influence of the sensor locations $\boldsymbol{s}_j, \boldsymbol{s}_{j+1} \in \mathbf{S}_k$. The influence of the particular sensor s_j to the reward of the data collected from s_i is computed as a part of the circle with the reward radius $\xi(s_i)$ that is inside the circle with the correlation radius $\chi(s_j)$ centered at $\boldsymbol{s_j}$. Such a covered part of the reward circle of the sensor s_i is computed for all the sensors in $\mathbf{S}_k$ and the expected information gain provided by the sensor measurements at s_i is decreased according to the ratio of the not covered portion of the reward circle $\xi(s_i)$ to the length of the complete circumference of the circle $\xi(s_i)$.

Each sensor location $\boldsymbol{s}_i \in \mathbf{S}$ is associated with the default reward $r(s_i)$ and two radii defining two circles centered at $\boldsymbol{s}_i$ that are called the correlation radius $\chi(s_i)$ and reward radius $\xi(s_i)$ (formerly the penalty radius in [34]). The circles are further referred as the correlation circle and reward circle with the particular radii $\chi(s_i)$ and $\xi(s_i)$, respectively. The geometrical relations of the radii are depicted in Fig. 1, where the default reward $r(s_i)$ of the sensor $s_i \notin \mathbf{S}_k$ is decreased according to the influence of the data collected from the sensors $s_j, s_{j+1} \in \mathbf{S}_k$. The influence is computed as the union of the covered parts of the reward circle of s_i by the correlation circles of the sensors s_j and s_{j+1}.

Let the total circumference of the reward circle with the radius $\xi(s_i)$ be $circ(\xi(s_i))$, the selected sensors be $\mathbf{S}_k$, the neighboring sensors of the sensor $s_i \notin \mathbf{S}_k$ in the graph $G(V, E)$ be $\mathbf{N}_i$, and the default reward of s_i be $r(s_i)$. The reward of s_i can be decreased because of correlation with the data provided by the sensors $\mathbf{N}_i$ that are collected by the current data collection path. The updated value of $r(s_i)$ with respect to $\mathbf{S}_k$ is determined as

$$r_{\mathbf{S}_k}(s_i) = \left(1 - \frac{\mathcal{L}(\xi(s_i), \mathbf{N}_i \bigcap \mathbf{S}_k)}{\mathrm{circ}(\xi(s_i)}\right) r(s_i), \tag{14}$$

where $\mathcal{L}(\xi(s_i), \mathbf{N}_i \bigcap \mathbf{S}_k)$ is the length of the union of covered parts of the reward circle $\xi(s_i)$ by the correlations circles of the influencing sensors selected in $\mathbf{S}_k$, i.e., circles of the sensors $s_j \in \mathbf{N}_i \bigcap \mathbf{S}_k$ with the radii $\chi(s_j)$ centered at $\boldsymbol{s}_j$.

Individual values of the correlation and reward radii (circles) can be set for each particular sensor. The model (14) can be then utilized during the solution of the PCTSP and OP to update the rewards of all sensors not currently selected in $\mathbf{S}_k$ whenever $\mathbf{S}_k$ is changed. The objective functions of the PCTSP and CEPCTSP, i.e., (1) and (5), respectively, include penalties (scaled values of the rewards) only for the sensors in $\mathbf{S} \setminus \mathbf{S}_k$. Since the rewards of $\mathbf{S}_k$ are not considered, it is not necessary to make any adjustments in the formulations of Problem 3.1 and Problem 3.2. The only needed calculation is the sum of penalties that can be influenced by the data collected from the selected $\mathbf{S}_k$ because of (14).

The sums of rewards in the OP (8) and CEOP (10) are computed using only the sensors $\mathbf{S}_k$ selected for data collection. Therefore, it is necessary to include the model (14) into the solution cost $R(\mathbf{S}_k)$ as the sum of the total collected rewards should also include the rewards collected as a result of the spatial correlation of $\mathbf{S}_k$ to $\mathbf{S} \setminus \mathbf{S}_k$, and thus the objective function $R(\mathbf{S}_k)$ is computed as

$$R(\mathbf{S}_k) = \sum_{s_i \in \mathbf{S}_k} r(s_i) + \sum_{s_j \in \mathbf{S} \setminus \mathbf{S}_k} \left(r(s_j) - r_{\mathbf{S}_k}(s_j)\right), \tag{15}$$

where $r_{\mathbf{S}_k}(s_j)$ is computed according to (14). Notice, when $\chi(s_i)$ is zero for all the sensors, the second term of (15) is zero and the spatial correlation between the measurements is not considered.

4. GSOA-based Data Collection Path Planning

The herein studied data collection path planning is addressed by the GSOA [19] which is a variant of the unsupervised learning network based on the principles of self-organizing map (SOM) for the TSP. The GSOA is an array of nodes $\mathcal{N} = \{\nu_1, \ldots, \nu_M\}$ that represents points in the problem space, i.e., $\boldsymbol{\nu} \in \mathbb{R}^2$. The connected nodes form a ring which represents the requested data collection path that evolves during the unsupervised learning of the GSOA. Each node $\nu \in \mathcal{N}$ is further associated with the particular sensor $\nu.\boldsymbol{s}$ and the corresponding waypoint location $\nu.\boldsymbol{p}$ at which data from s can be retrieved within δ communication radius, i.e., the waypoint location is inside the δ-disk centered at $\boldsymbol{s}$. A similar notation as for the sensors is used for the nodes, and ν denotes the node, and its location is $\boldsymbol{\nu}$.

The learning procedure is an iterative adaptation of the GSOA to the sensors $\mathbf{S}$ in a finite number of learning epochs. In each learning epoch, a new node ν^* may be added to $\mathcal{N}$ for each sensor $s \in \mathbf{S}$ and ν^* can be then adapted towards s. The sensors $\mathbf{S}$ are considered in a random order for each learning epoch to avoid local optima. For each sensor s a new node ν^* is determined together with the waypoint location $\nu^*.\boldsymbol{p}$ using the winner node selection, see Fig. 2a. Then, ν^* together with its neighbouring nodes in the ring are adapted towards the waypoint location $\nu^*.\boldsymbol{p}$, i.e., their positions are adjusted to "move" towards the waypoint

$$\boldsymbol{\nu}' = \boldsymbol{\nu} + \mu f(\sigma, d)(\nu^*.\boldsymbol{p} - \boldsymbol{\nu}) \tag{16}$$

with the power of the adaptation defined by the neighbouring function

$$f(\sigma, d) = \begin{cases} e^{-\frac{d^2}{\sigma^2}} & \text{for } d < 0.2M \\ 0 & \text{otherwise} \end{cases} , \tag{17}$$

where M is the current number of nodes in $\mathcal{N}$ and d is the distance of the node ν from ν^* in the number of nodes in the ring. Finally, all nonwinning nodes are removed from $\mathcal{N}$ at the end of each learning epoch to keep the number of nodes in $\mathcal{N}$ balanced with the number of sensors.

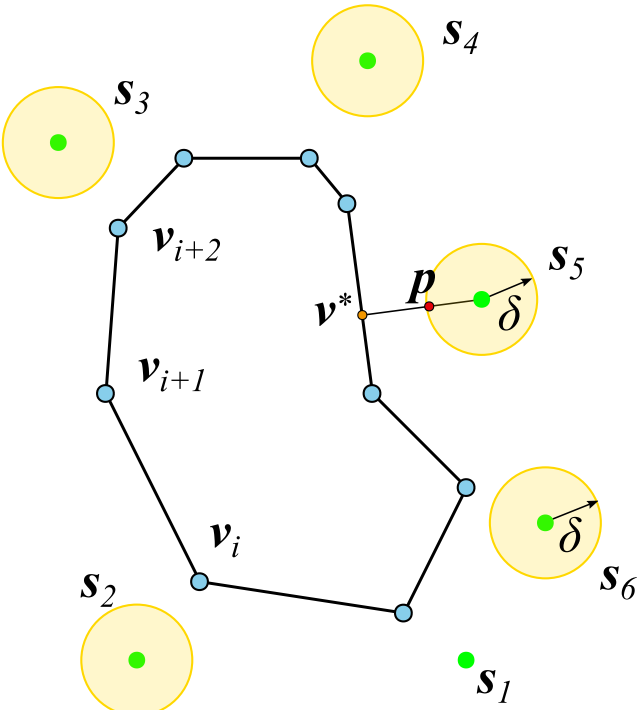

(a) Winner node selection

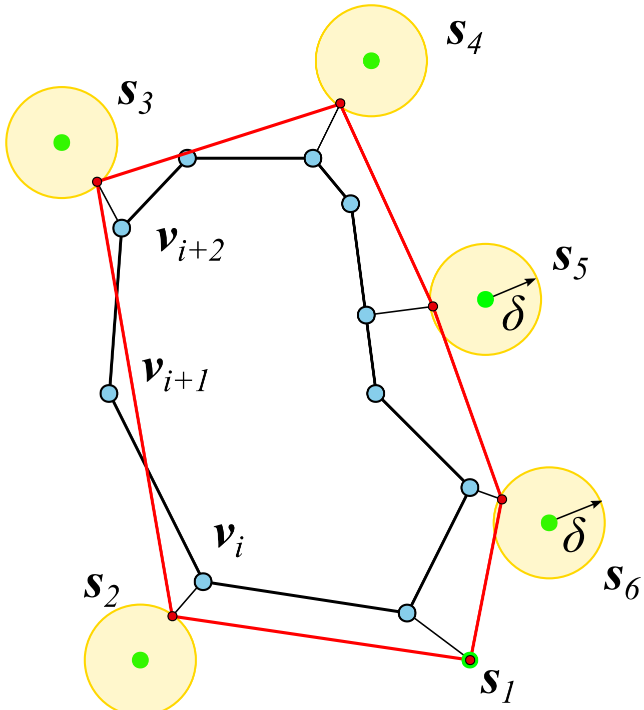

(b) Path represented by $\mathcal{N}$

Figure 2: Demonstration of the principle of winner node selection (on the left) where the closest point of the ring of connected nodes $\mathcal{N}$ to the particular sensor s_5 is determined as the position of the new node $\boldsymbol{\nu}^*$ together with the particular waypoint $\boldsymbol{p}$ to retrieve data from s_5 within δ communication range. (on the right) The ring of nodes $\mathcal{N}$ defines the order of visits to the sensors associated to the nodes and the connected waypoints $\boldsymbol{p}$ form the requested data collection path that is shown in red. The nodes are shown as small blue disks, and the sensor locations are shown as small green disks with the particular surrounding perimeter according to the communication range δ. The images are adapted from [19] where the GSOA for the CETSP is introduced.

The array of nodes $\mathcal{N}$ represents a ring in $\mathbb{R}^2$ and the sequence of nodes in the ring defines the order of visits to the sensors associated with the nodes. Moreover, the sequence of nodes defined by the array $\mathcal{N}$ and the associated waypoint locations to the nodes can be used to quickly construct the data collection path from which data from the selected sensors can be retrieved. This is the main benefit of the GSOA over the SOM-based solvers for the TSP because it allows to trade-off the visitation of the particular sensor and the path length in a solution of the PCTSP or to explicitly address the limited travel budget in the OP. Besides, the growing structure allows to easily adjust the number of nodes according to the selected sensors. The winner selection and an example of the path represented by the ring are depicted in Fig. 2. Note that in the GSOA, a feasible solution is available at the end of each learning epoch, and therefore, there are not issues with the convergence, and the GSOA has anytime property, see detailed discussion in [19].

The GSOA as it has been introduced for solving the TSP and CETSP in [19] can be almost directly used in the solution of the CEPCTSP and CEOP. There are two main adjustments needed to solve these problems. The first is the initialization of the ring $\mathcal{N}$, where the ring is initialized to a single node located at $\boldsymbol{s}_1$, which is the same as for the TSP; however, an open path with the initial location $\boldsymbol{s}_1$ and terminal location $\boldsymbol{s}_n$ is requested in the OP. Therefore, the GSOA is initialized as two nodes ν_1 and ν_{end} that are never adapted nor removed from the array. Besides, the neighboring function (17) has to respect the open path in the solution of the OP and CEOP.

The second adjustment is related to trade-off the path length and rewards of the not visited sensors in the PCTSP and to satisfy the budget limit $\mathrm{T}_{\max}$ in the OP. Both these aspects are addressed by the same way as the conditional adapt of the GSOA to the particular sensors. New nodes are determined for all sensors in every learning epoch, but the new node is inserted into the GSOA only if certain criteria are met. In the case of the PCTSP, the adaptation is performed only if the distance of the new node $\boldsymbol{\nu}^*$ and its waypoint location $\nu^*.\boldsymbol{p}$ is shorter than the penalty (reward) to not collect data from s, i.e., the adaptation is performed only if $\|(\boldsymbol{\nu}^*, \nu^*.\boldsymbol{p})\| \leq \lambda r(\nu^*.s)$. However, for the first learning epoch, it is likely the case that new nodes are very far from the sensors, and thus this rule is not active for the first learning epoch.

For the OP, the adaptation of the ring is performed only if the path represented by the ring after the adaptation would be shorter than $\mathrm{T}_{\max}$ [31]. Because the nodes in $\mathcal{N}$ have associated waypoints, this can be evaluated as follows. Let the current epoch be i, the current ring $\mathcal{N}$ have M nodes and represent a path with the length L, ν^* be the current winner node, ν_{prev} be the first neighboring node of ν^* in the direction to ν_1 that has been added to $\mathcal{N}$ in the epoch i (or ν_1 if such a node has not been added yet), and ν_{next} be similarly the first neighboring node of ν^* towards ν_M added in the current epoch (or ν_{end} if such a node has not been added yet), then ν^* is kept in $\mathcal{N}$ and the ring is adapted towards the respective sensors only if

$$L - d_p(\nu_{prev}, \nu_{next}) + d_p(\nu_{prev}, \nu^*) + d_p(\nu^*, \nu_{next}) \leq \mathrm{T}_{\max}, \tag{18}$$

where $d_p(\nu_i, \nu_j)$ is the distance between the waypoints associated to ν_i and ν_j, i.e.,

$$d_p(\nu_i, \nu_j) = \|(\nu_i.\boldsymbol{p}, \nu_j.\boldsymbol{p})\|. \tag{19}$$

If the conditional adaptation is not performed, the new node ν^* is discarded and the ring is not adapted towards the particular s.

Beside of these conditions for the actual adaptation of the nodes to the particular sensor location, it is desirable to consider the rewards associated with the sensors. In [31], it is proposed to adjust the power of adaptation (16) according to the reward of the sensor towards which the ring is adapted. This is especially suitable for solving instances of the OP, where the preference of highly rewarding sensors is crucial in finding high-quality solutions. Therefore, the adaptation has the form

$$\boldsymbol{\nu}' = \boldsymbol{\nu} + R(s)\mu f(\sigma, d)(\nu^*.\boldsymbol{p} - \boldsymbol{\nu}), \tag{20}$$

where $R(s)$ is the normalized reward of the sensor s computed as $R(s) = r(s)/R_{max}$ for

$$R_{max} = \max_{s \in \mathbf{S}} r(s). \tag{21}$$

The value of the sensor reward $r(s)$ is a subject of change when spatial correlations are considered, but since the learning is performed in several iterations, the updated rewards can be directly utilized whenever the network is

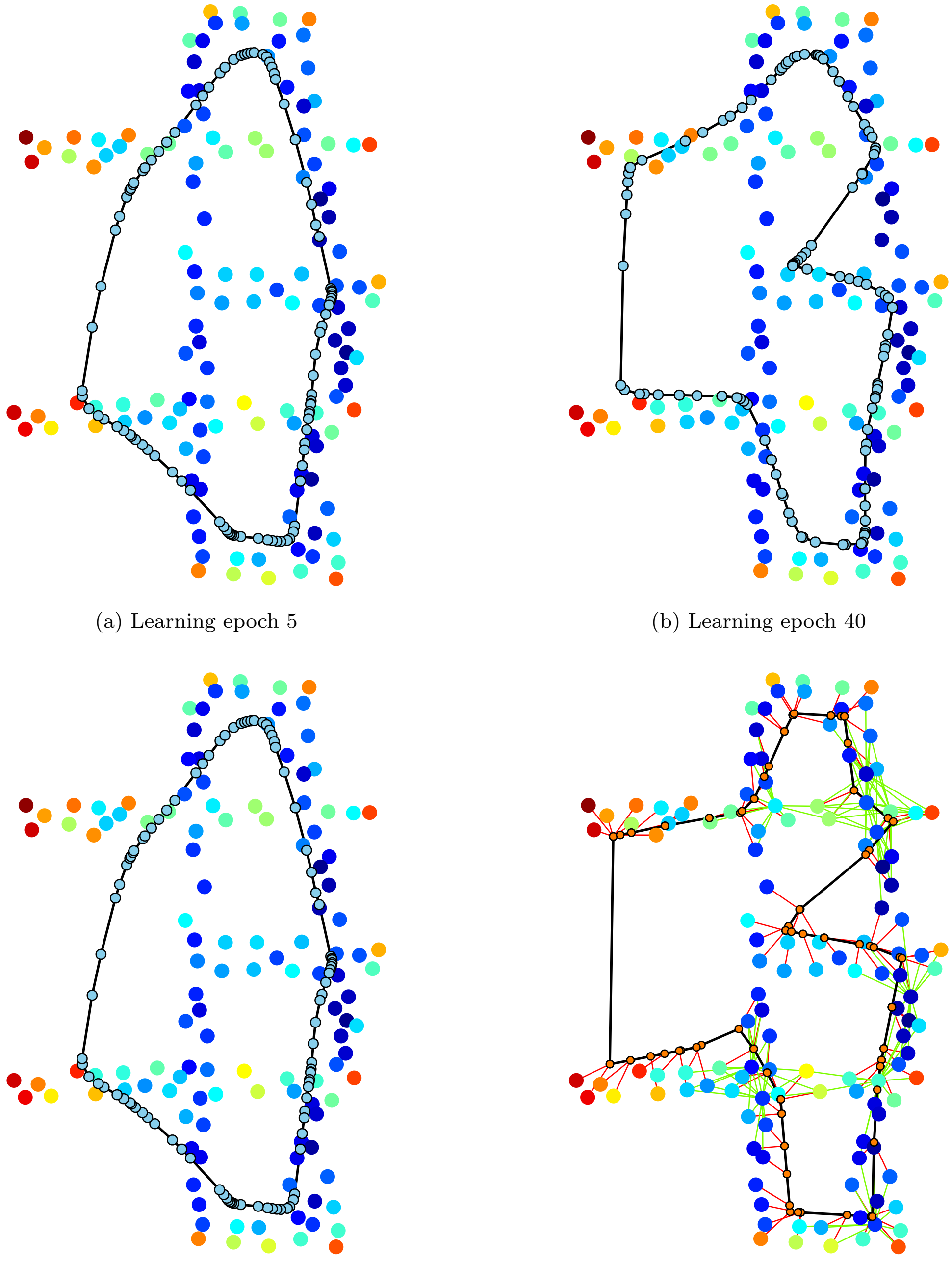

(a) Learning epoch 5

(b) Learning epoch 40

(c) Learning epoch 70

(d) Final found solution

Figure 3: Evolution of the GSOA in a solution of the CEPCTSP with spatial correlations. The nodes are visualized as small light blue disks connected to the ring. The sensors are shown as colored disks where sensors with high rewards (penalties) are in red and sensors with low rewards are in blue. The final solution is the data collection path connecting the waypoints shown as small orange disks. The red segments connecting waypoints with the sensors denote the communication range δ. The spatial correlations are shown by connecting the influencing sensors by green segments. Thus each sensor s_i from which data are directly collected are connected with the N_i neighbouring nodes that are not selected in the solution, but a part of the information about the locations is included in data collected from s_i.

adapted to the sensors, and the sensor is selected to be part of the data collection path for the current learning epoch.

The adaptation (20) is beneficial for solving the OP, but it does not provide an added value in a solution of the PCTSP. Although it negligibly increases the solution cost, according to the performed evaluations it increases computational cost noticeably because of slower convergence, and therefore, the standard adaptation (16) is rather

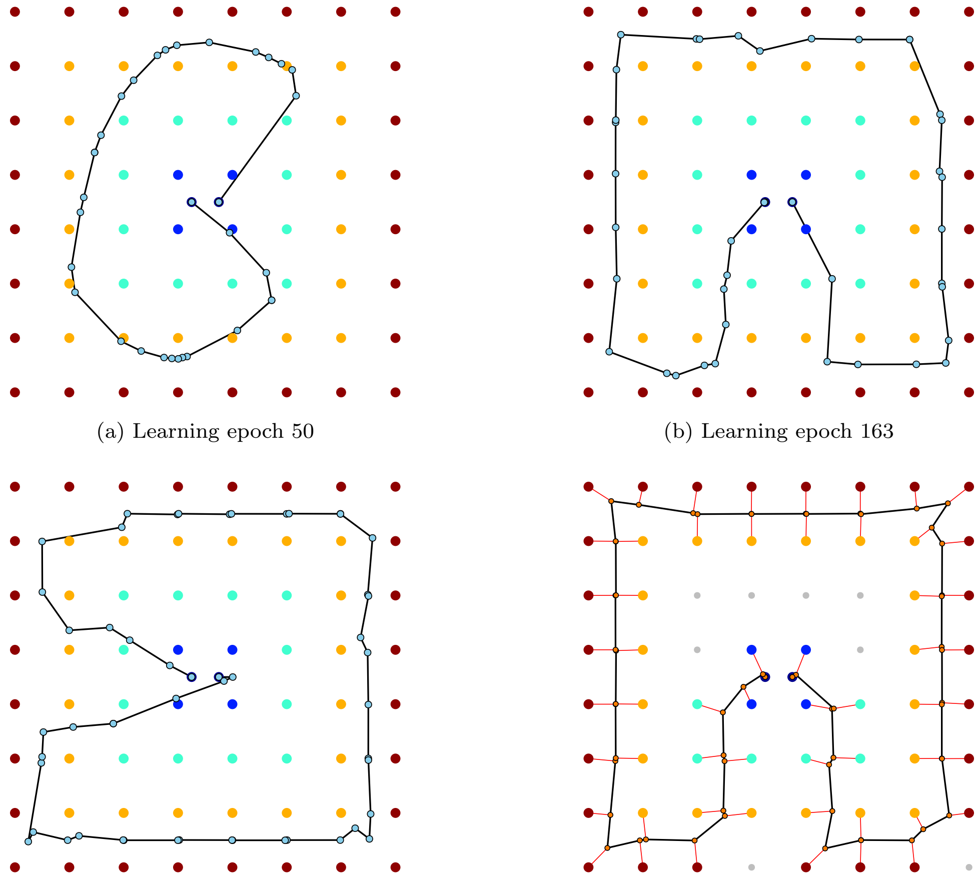

(a) Learning epoch 50 (b) Learning epoch 163

(c) Learning epoch 460 (d) Final found solution

Figure 4: Evolution of the GSOA in a solution of the CEOP instance called Set 66 with the travel budget $\mathrm{T}_{\max} = 60$, communication range $\delta = 1.0$, and $\chi = 0$, i.e., without the spatial correlations. The visualization follows the same color schema as in Fig. 3. A new solution is determined every learning epoch, and therefore, the GSOA is performing as a stochastic search where the best solution found so far is maintained during the learning.

preferred for solving the PCTSP.

In addition to the conditional adaptation, it is suggested in [31] to support adaptation by avoiding saturation of the path length close to $\mathrm{T}_{\max}$ and up to two nodes of $\mathcal{N}$ may be removed from the array if the length of the path represented by the array would be longer than $\mathrm{T}_{\max}$ after adding new sensor to $\mathbf{S}_k$. These two nodes represent the node $\nu_f \in \mathcal{N}$ with the longest distance to its waypoint $\nu_f.\boldsymbol{p}$ and the node $\nu_l \in \mathcal{N}$ which is the node associated to the sensor $\nu_l.s$ with the lowest reward. Both the nodes ν_f and ν_l can be therefore removed from $\mathcal{N}$ during the winner node selection. However, if the ring is not adapted to the sensor because of (18), the deletion of these nodes is rolled-back, i.e., the ring is set to the state before the winner node selection.

Examples of the proposed GSOA for data collection planning in a solution of the CEPCTSP with spatial correlations is shown in Fig. 3. The solution follows the GSOA for the CETSP [19], and the network quickly converges to a stable solution which does not evolve with further learning epochs. Thus, solutions of the CEPCTSP instances reported in Section 5 are found in tens of learning epochs and typically in less than one hundred epochs. An example of the GSOA evolution in solving the CEOP instance Set 66 is presented in Fig. 4.

An overview of the GSOA learning procedure is depicted in Fig. 7 where the particular modifications to solve PCTSP and OP formulations of the data collection path planning algorithms are highlighted. The additional procedure for removing nodes ν_f and ν_l in solving instances of the OP is depicted in Fig. 6.

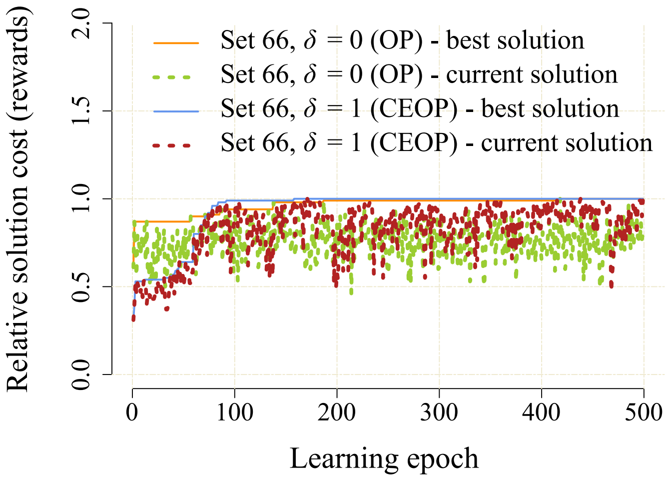

Figure 5: Evolution of the relative solution cost (sum of the rewards) in particular learning epochs to the final solution cost in solving the Set 66 instance of the OP and CEOP with $\mathrm{T_{max}} = 60$ for $\delta = 0$ and $\delta = 1$, respectively.

Procedure remove_nodes($\mathcal{N}, s, \nu^*$):

1. Get all winner nodes of the current epoch $\mathcal{N}_{win} \leftarrow$ winners($\mathcal{N} \setminus \{\nu_1, \nu_{end}\}$).
2. Determine the winner node ν_f which has the longest distance to its associated waypoint $\nu_f.\boldsymbol{p}$

$$\nu_f = \mathrm{argmax}_{\nu \in \mathcal{N}_{win}} \|(\nu, \nu.\boldsymbol{p})\| \,. \tag{22}$$

3. Determine the winner ν_l which associated sensor location $\nu_l.s$ has the lowest reward

$$\nu_l = \mathrm{argmin}_{\nu \in \mathcal{N}_{win}} r(\nu.s). \tag{23}$$

4. `If` the expected path length after the adaptation of ν^* would be longer than $\mathrm{T_{max}}$.
   - `If` $r(\nu_f.s) < r(s) \wedge \|(\boldsymbol{\nu}_f, \nu_f.\boldsymbol{s}\| > \|(\boldsymbol{\nu}^*, \boldsymbol{s})\|$ `Then` remove ν_f from the ring $\mathcal{N} \leftarrow \mathcal{N} \setminus \{\nu_f\}$.
   - `If` $r(\nu_l.s) < r(s) \wedge \|(\boldsymbol{\nu}_l, \nu_l.\boldsymbol{s}\| > \|(\boldsymbol{\nu}^*, \boldsymbol{s})\|$ `Then` remove ν_l from the ring $\mathcal{N} \leftarrow \mathcal{N} \setminus \{\nu_l\}$.
5. return($\mathcal{N}$).

Figure 6: Removing of not promising nodes from the current ring to support adaptation of the current winner node ν^* and satisfying the limited travel budget $\mathrm{T_{max}}$ in a solution of the OP. The procedure has been originally proposed in [31].

A new solution is determined in every learning epoch in solving the OP. It is because new nodes are added to the ring for every considered sensor which is selected according to (18). Since only the newly added nodes in the current learning epoch are preserved for the next epoch, and sensors are evaluated in a random order, the learning procedure can be considered as a stochastic search. However, it is not an issue as the best solution found so far is maintained (Line 25 of the GSOA algorithm depicted in Fig. 7) and it can only improve over the time. An evolution of the solution cost (the sum of the collected rewards R) found in the particular learning epochs and the final best-found solution are depicted in Fig. 5. It can be noticed that a solution close to the final solution is found relatively quickly in around 200 learning epochs, but a bit better solution can be found in additional epochs. Because the computational requirements of the GSOA are relatively very low, see the results reported in Section 5, the maximal number of learning epochs is set to $i_{max} = 500$. The initial values of the learning parameters are set at Line 2 of the GSOA algorithm in Fig. 7. The particular values have been found empirically and they originate from the evaluation reported in [50]. Although the performance of the GSOA can be tuned by adjusting the parameters'

GSOA for data collection planning formulated as the Close Enough PCTSP and OP

Input: $\mathbf{S} = \{\boldsymbol{s}_1, \ldots, \boldsymbol{s}_n\}$ – a set of sensor locations to be visited, each with particular disk-shaped δ-neighborhood and default reward value r_i. For the spatially correlated measurements, each sensor $s_i \in \mathbf{S}$ is further associated with the correlation radius χ_i and reward radius ξ_i.

Input: $\mathrm{T}_{\max}$ – the maximal allowed travel budget in the case of solving the OP.

Input: i_{max} – the maximal number of learning epochs, i.e., $i_{max} \leftarrow 150$ for solving the PCTSP and $i_{max} \leftarrow 500$ for solving the OP.

Output: $(\mathbf{S}_k,\Sigma_k,\mathbf{P}_k)$ – $\mathbf{S}_k$ is a set of k selected sensors, Σ_k is the order of visits to the sensors, $\mathbf{P}_k$ is the array of the corresponding waypoint locations at which data from $\mathbf{S}_k$ can be retrieved.

▷ *Initialization*

Set the learning parameters: the initial value of the learning gain $\sigma \leftarrow 10$, the gain decreasing rate $\alpha \leftarrow 0.0005$, and the learning rate $\mu \leftarrow 0.6$.

► **if solving the PCTSP**: $\mathcal{N} \leftarrow \{\nu_1\}$ such that $\boldsymbol{\nu}_1 = \boldsymbol{s}_1$; ν_1 is always adapted towards s_1 in every learning epoch.

► **if solving the OP**: $\mathcal{N} \leftarrow \{\nu_1, \nu_{end}\}$ such that $\boldsymbol{\nu}_1 = \boldsymbol{s_1}$, $\boldsymbol{\nu}_{end} = \boldsymbol{s}_n$, and ν_1 and ν_{end} are never changed nor removed from $\mathcal{N}$ during the learning.

$i_{max} \leftarrow \min(i_{max}, 1/\alpha)$ // ensure σ will always be above 0

$i \leftarrow 1$ // set the learning epoch counter

while $i \leq i_{max}$ $\wedge$ *solution is changing* **do**

  ▷ *Learning epoch*

  foreach s *in a random permutation of* $\mathbf{S}$ **do**

    $\nu^*(\boldsymbol{\nu}^*, \nu^*.\boldsymbol{p}) \leftarrow \text{determine\_winner}(\mathcal{N}, s, \delta_s)$ // Determine the winner node for s according to Fig. 2

    ► **if solving the OP then**

      $\mathcal{N}' \leftarrow \mathcal{N}$ // save the ring for the case the adaptation would fail because of $\mathrm{T}_{\max}$

      $\mathcal{N} \leftarrow \text{remove\_nodes}(\mathcal{N}, s, \nu^*)$ // remove nodes to possibly fit the path length to $\mathrm{T}_{\max}$, see Fig. 6

    ▷ *Conditional adapt*

    if $\begin{cases} (\ i=1\ )\ \vee\ (\ \|(\boldsymbol{\nu}^*, \nu.\boldsymbol{p})\| \leq \lambda r(s)\ ) & \text{►}\textbf{for solving the PCTSP} \\ \text{Condition (18) holds} & \text{►}\textbf{for solving the OP} \end{cases}$ **then**

      $\mathcal{N} \leftarrow \text{insert\_winner}(\mathcal{N}, \nu^*)$

      foreach *node* $\nu \in \mathcal{N}$ *in the d-neighborhood of the node* ν^* *such that* $0 \leq d \leq 0.2M$ **do**

        Adapt ν towards $\nu^*.\boldsymbol{p}$ using (16) **for solving the PCTSP** or using (20) **for solving the OP** with the neighborhood function (17).

    else

      ► **if solving the OP**: $\mathcal{N} \leftarrow \mathcal{N}'$ // revert changes made by $\text{remove\_nodes}(\mathcal{N}, s, \nu^*)$

  ▷ *Update the ring and the best solution found so far*

  $\mathcal{N} \leftarrow \text{regenerate}(\mathcal{N})$ // remove all not winning nodes from $\mathcal{N}$

  $i \leftarrow i + 1$ // update the epoch counter

  $\sigma \leftarrow (1 - i\alpha)\sigma$ // decrease the learning gain

  Determine a solution $\mathbf{S}'_k$ and Σ'_k with the corresponding waypoints $\mathbf{P}'_k$ by traversing the current ring of nodes. **if** $\begin{cases} C(\mathbf{S}'_k, \Sigma'_k, \mathbf{P}'_k) < C(\mathbf{S}_k, \Sigma_k, \mathbf{P}_k) & \text{►}\textbf{for solving the PCTSP} \\ (R(\mathbf{S}'_k, \Sigma'_k, \mathbf{P}'_k) > R(\mathbf{S}_k, \Sigma_k, \mathbf{P}_k)) & \text{►}\textbf{for solving the OP} \end{cases}$ **then**

    $(\mathbf{S}_k, \Sigma_k, \mathbf{P}_k) \leftarrow (\mathbf{S}'_k, \Sigma'_k, \mathbf{P}'_k)$ // update the best solution found so far

return $(\mathbf{S}_k, \Sigma_k, \mathbf{P}_k)$

Figure 7: An overview of the GSOA for solving the PCTSP and OP; both also in the Close Enough variant as the CEPCTSP and the CEOP. For the solution of the OP, nodes ν_f and ν_l can be removed from the ring using the $\text{remove\_nodes}(\mathcal{N}, s, \nu^*)$ procedure that is depicted in Fig. 6.

values, the performance is only slightly changing, and therefore, they are considered as constants.

Also note that for small budgets $\mathrm{T}_{\max}$ it does not make sense to consider sensor locations that are unreachable. Therefore, sensors for which $\mathrm{T}_{\max}$ does not allow to travel from s_1 and returning to s_n are not considered in the

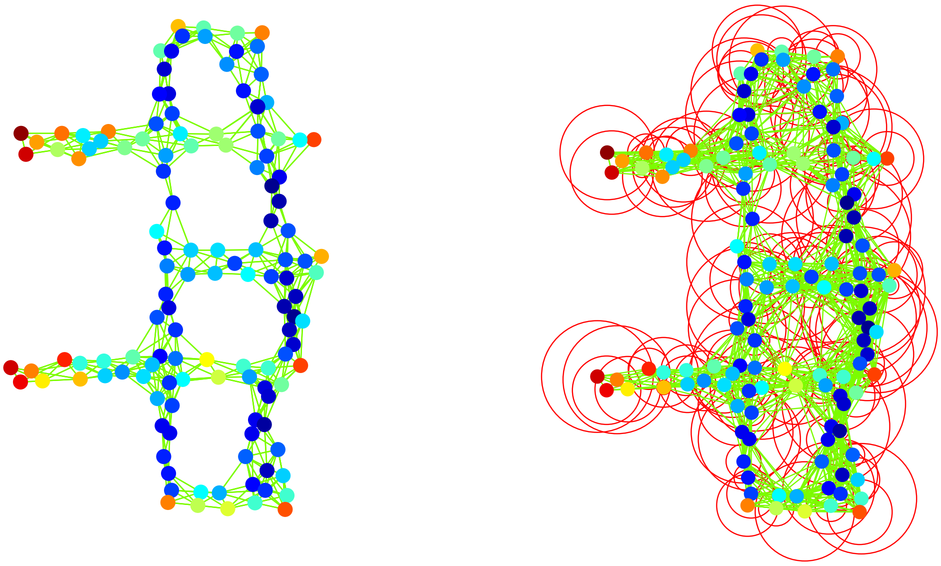

(a) OOI scenario, $\xi = 50$ km, $\chi = 25$ km, and $\delta = 0$ km

(b) OOI scenario, $\xi = 50$ km, $\chi = 100$ km, and $0 \leq \delta \leq 100$ km

Figure 8: Examples of the solved OOI scenarios with spatial correlations. The sensors are visualized as small disks with the color according to the associated rewards (red for high reward values and blue for low reward values). The green segments connect sensors with spatial correlations of the measured data, i.e., a sensor is connected with another sensor if data collected from one sensor also provides some information that can be collected from another sensor. The individual communication radius per each sensor is shown as the red circle around the sensor locations (on the right).

solution of the particular OP instance, similarly to heuristic approaches, e.g., 4-phase algorithm [51].

5. Results

The proposed GSOA for data collection path planning has been evaluated in a series of scenarios where the data collection planning problem is addressed as one of the variants of the PCTSP and OP. The performance of the GSOA in solving the PCTSP is performed in the OOI scenario that has been introduced in [33], which is motivated by autonomous data collection from a set of 128 sampling stations located on an ocean floor. Several instances of the PCTSP and CEPCTSP are created from the OOI scenario also considering correlations between the sensors. An example of two instances with visualization of the spatial correlations and individual communication radius per each sensor are depicted in Fig. 8.

On the other hand, scenarios used for evaluation of the GSOA in OP instances are created from the standard benchmarks proposed in [52]. In particular, the problems called Set 64 and Set 66 are considered because they represent more complex problems than the other standard OP benchmarks available at [53]. In addition to these existing benchmarks, the OOI scenario utilized in the evaluation of the PCTSP [33] and visualized in Fig. 8 is considered for creation of new OP instances with the two additional locations for the requested initial and terminal position of the vehicle with the total number of locations 130. The original OOI scenario is proportionaly scaled down about the factor 10 to make it close to the standard Set 64 and Set 66, and the new OP dataset is called Set 130[2]. Each OP scenario is further defined by the particular value of the travel budget T_{max} (see [53] or the further reported results),

[2]The OP instances of the Set 130 are available at `https://purl.org/faigl/op`.

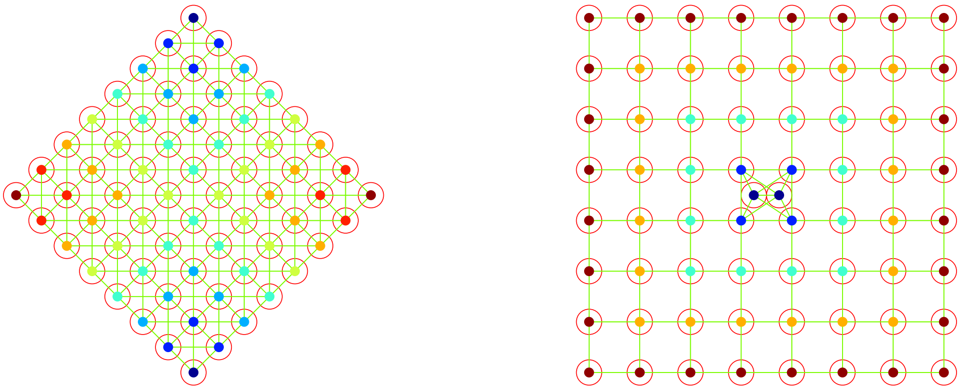

(a) Set 64 (b) Set 66

Figure 9: Instances of the OP scenarios Set 64 and Set 66 both with the reward radius $\xi = 0.5$, the correlation radius $\chi = 2$, and the identical communication radius for all the sensors $\delta = 0.5$. The green line segments denote nearby correlated sensors.

where for increasing budget, more sensors can be visited and the problem can be considered closer to the TSP. The newly introduced Set 130 is accompanied with the travel budget $\mathrm{T_{max}} = \{50, 100, 150, 200, 250, 300, 350, 400, 410\}$. The problems are also used to create instances of the CEOP with particularly specified communication radii δ. An example of the particular instances of the Set 64 and Set 66 with communication radius $\delta = 0.5$ is depicted in Fig. 9 to show the dimensions of the problem and spatial relations. Besides, selected instances are further

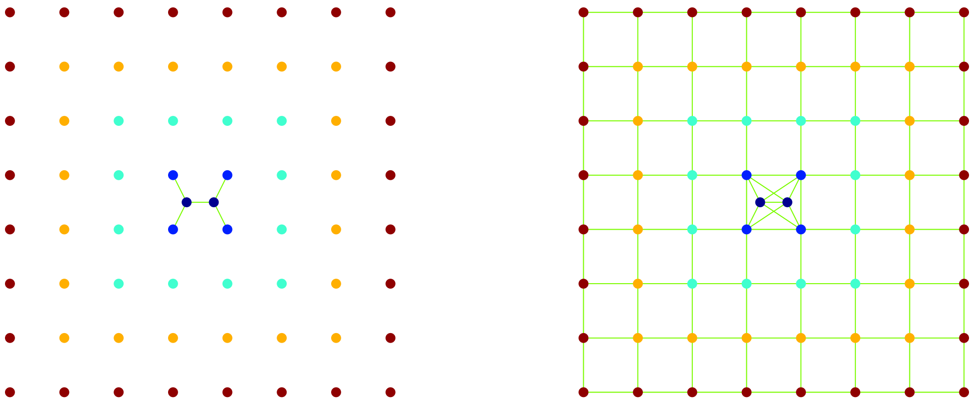

(a) Set 66, $\chi = 1$ (b) Set 66, $\chi = 2$

Figure 10: Examples of the created OP scenarios with spatial correlations using the reward radius $\xi = 0.5$ and correlation radius χ. The green line segments is a visualization of the spatially correlated sensors.

used in evaluation of spatial correlations that is studied for different values of the correlation radius χ and reward radius ξ. Influence of different correlation radii to the influencing nearby sensors in Set 64 scenarios with zero communication radius is demonstrated in Fig. 10. An overview of the Set 130 is visualized in solutions shown in Fig. 21 and Fig. 22.

The PCTSP also with the non-zero communication radius δ as the CEPCTSP have been already addressed by the unsupervised learning together with the comparison with traditional combinatorial heuristics in [54, 33] and with spatial correlations firstly tackled in [34]. Thus, the herein presented evaluation results on the PCTSP is mainly to show the influence of different correlation radii and performance of the GSOA in solving this type of data collection planning formulation.

The focus of the presented performance evaluation is on the novel GSOA-based approach to the OP and CEOP together with the study of the influence of spatial correlations to the sum of the collected rewards to demonstrate the capability of the proposed GSOA solution to exploit the non-zero communication radius and correlation radius. The first SOM-based unsupervised learning approach to the CEOP has been presented in [30] and its improved version in [31] together with the comparison to the existing combinatorial heuristics in the standard OP benchmarks [53]. Therefore, the proposed GSOA solution is compared with the approaches [30] and [31] that are further denoted as SOM v1 and SOM v2, respectively. Besides, the results in standard OP instances are compared with one of the best performing traditional heuristic [52] denoted as the CGW and one of the very first heuristics for the OP called 4-phase [51] that has been reimplemented to compare computational requirements of the combinatorial heuristic with unsupervised learning based approaches. Since the only existing available solvers for the CEOP without spatial correlations are those based on unsupervised learning, the performance evaluation is presented for selected CEOP instances. Finally, the only currently available solution for the CEOP with spatial correlations is the proposed GSOA-based method, and thus the evaluation is focused on the study the influence of the correlation radius and communication radius to the solution cost and computational requirements.

The used parameters of the SOM-based solvers are set as they are reported in [30] and [31]. For the proposed GSOA-based solvers the same values of the initial learning gain σ, the gain decreasing rate α, and the learning rate μ as presented in Fig. 7 are used for both problems: the PCTSP and OP. The only difference is that for solving the PCTSP, the maximal number of learning epochs is set to $i_{max} = 150$ because the network usually converges in tens of epochs. For the solution of the OP, i_{max} is set to $i_{max} = 500$ as the learning is de facto stochastic search.

All the unsupervised learning and 4-phase [51] algorithms have been implemented in C++ and run within the same computational environment using a single core of the Intel Core i7-6700K processor running at 4 GHz. The SOM-based and GSOA-based algorithms are stochastic, and therefore, the presented results are computed from 20 trials per each particular problem instance that is defined by the scenario, reward, correlation, and communication radii and in the case of the OP also the travel budget $\mathrm{T}_{\mathrm{max}}$.

The performance indicators are the solution quality and the required computational time. The solution quality is reported as the average cost of the solution C (accompanied by the standard deviation) for the PCTSP instances. In the case of the OP, the solution quality is reported as the average collected sum of the rewards R that is rounded to integers as the rewards are integer values in Set 64 and Set 66 [53]. Besides, following the literature on the OP [55, 56], the quality is also reported as the relative percentage error (RPE) computed as

$$\mathrm{RPE} = \frac{R_{opt} - R}{R_{opt}} \cdot 100\%, \tag{24}$$

where R is the best solution among the performed trials and R_{opt} is the optimal solution for the particular instance reported in the literature [56, 57, 28] and also found by the ILP-based solver for the OP. Besides, the algorithm robustness over the performed trials is reported as the average relative percentage error (ARPE) [56]

$$\mathrm{ARPE} = \frac{R_{opt} - R_{avg}}{R_{opt}} \cdot 100\%, \tag{25}$$

where R_{avg} is the average sum of the collected rewards among the trials of the particular problem instance. For the newly introduced Set 130, the best solution found among of all evaluated algorithms is considered as the reference solution R_{ref} instead of R_{opt} because the optimal solution is not available.

The required computational time $\mathrm{T}_{\mathrm{CPU}}$ is reported as the average real computational time that is presented in milliseconds due to the computational efficiency of the proposed GSOA and unsupervised learning approaches. The standard deviations are shown as error bars in the accompanied bar plots.

5.1. Close Enough PCTSP with Correlation Measurements

The performance of the proposed GSOA in the PCTSP instances, or more particularly in the CEPCTSP instances with spatial correlations, has been evaluated in OOI scenarios with different communication and correlation radii. The selected OOI scenarios represent data collection missions from an area about 450×700 km large performed by an autonomous underwater vehicle operating with a constant velocity 5 km/h [33]. The communication range δ is considered up to 20 km, i.e., $\delta \in \{0,\ 5,\ 10,\ 20\}$ in km, the reward radius $\xi = 25$ km, and the correlation radius is considered as $\chi \in \{0, 14, 35\}$ in km.

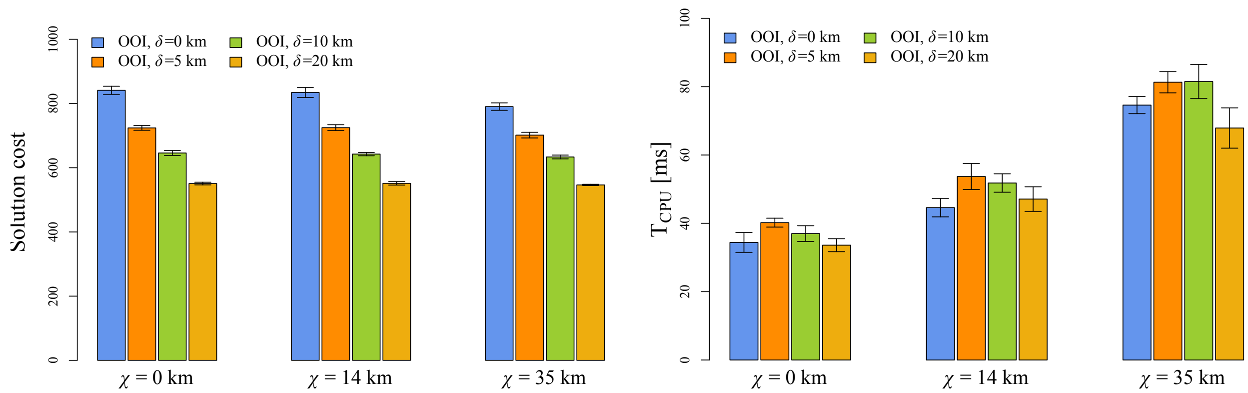

(a) Average solution cost (b) Average computational requirements

Figure 11: The average solution cost per each OOI scenario of the PCTSP with spatially correlated rewards (penalties) for the communication radius δ and correlation radius χ. The reward radius ξ of the distant based spatial correlation model is $\xi = 25$ km; however, the spatial correlations are enabled only for $\chi > 0$.

The average solution cost is depicted in Fig. 11a. It can be noticed that the increasing communication range δ has a significant positive influence on the solution cost. However, the benefit of exploiting spatial correlations is mostly noticeable for $\delta = 0$ and $\chi = 35$ km. The average computational requirements per solution of a single trial are depicted in Fig. 11b. In all cases, the solution is provided in less than one hundred milliseconds. The computational requirements are slightly increased with increasing communication range δ but from a certain distance, the convergence of the network is faster, and thus the learning needs less number of learning epochs. Regarding the spatial correlations, the learning procedure is noticeably more demanding for increased χ. It is because for a longer χ more sensors are in the influencing neighborhood set $\mathbf{N}_i$ and the evaluation of (14) is more computationally intensive.

For the particular case of the evaluated OOI scenarios, considering spatial correlations only slightly decreases the solution cost. In particular, for $\delta = 0$ the average solution cost C is $C = 841$ km for $\chi = 0$ km and it is $C = 790$ km for $\chi = 35$ km, which is noticeable but not directly visible in Fig. 11a. On the other hand, considering $\delta = 5$ km and $\chi = 0$ km, the average solution cost is significantly lower $C = 724$ km. Nevertheless, the proposed GSOA approach is capable of exploiting the spatial correlations between the measurements in benefit of the improved solution at the cost of increased computational requirements, which are about two times more demanding for $\chi = 35$ km than for $\chi = 0$ km.

5.2. GSOA in the Orienteering Problem

The performance of the novel GSOA-based solution of the OP has been evaluated using the standard OP benchmarks Set 64 and Set 66 [53] with 64 and 66 nodes, respectively, and with the travel budget $T_{\max}$ ranging from 15 to 80 and 130, respectively. The detail results are presented in Table 1 and Table 2. Besides, the OP instances for the Set 130 have been solved by the implemented 4-phase [51] heuristics and the unsupervised learning based approaches, and the results are reported in Table 3.

Table 1: Performance of the Proposed GSOA solver for the OP in Set 64

T_{max}	R_{opt}	CGW	4-phase [51]			SOM v1 [30]			SOM v2 [31]			**Proposed GSOA**		
		RPE	RPE	ARPE	T_{CPU}*	RPE	ARPE	T_{CPU}*	RPE	ARPE	T_{CPU}*	RPE	ARPE	T_{CPU}*
15	96	0.00	0.00	0.00	547.0	0.00	0.00	96.6	0.00	0.00	13.2	0.00	0.00	13.3
20	294	0.00	0.00	0.00	1 258.0	0.00	0.00	473.0	0.00	0.82	26.4	0.00	1.02	25.7
25	390	0.00	1.54	1.54	1 084.0	1.54	6.54	576.7	1.54	8.31	31.6	1.54	7.62	31.3
30	474	0.00	3.80	3.80	2 074.0	3.80	8.99	637.4	2.53	7.47	38.6	5.06	7.72	36.6
35	576	1.04	5.21	5.21	2 362.0	4.17	7.34	653.8	1.04	4.43	45.0	2.08	5.26	44.4
40	714	0.00	5.88	5.88	2 278.0	5.04	8.99	675.9	3.36	5.59	51.6	3.36	5.34	49.6
45	816	0.00	6.62	6.62	2 167.0	7.35	11.21	691.6	1.47	5.81	58.2	5.15	6.43	56.5
50	900	0.00	6.67	6.67	3 235.0	7.33	9.93	696.0	4.00	5.90	64.0	4.00	6.07	61.8
55	984	0.00	4.27	4.27	3 367.0	7.32	10.73	688.2	3.05	4.76	68.5	2.44	4.82	65.4
60	1 062	1.69	1.13	1.13	4 341.0	5.08	9.12	672.9	2.82	5.00	72.6	3.95	5.20	70.7
65	1 116	0.00	0.54	0.54	4 099.0	3.23	6.40	648.6	2.15	3.39	76.0	2.15	3.74	75.6
70	1 188	1.01	0.51	0.51	5 318.0	4.04	5.76	611.6	2.02	3.74	79.8	1.01	3.76	76.4
75	1 236	0.97	2.91	2.91	6 615.0	1.46	3.88	580.6	0.49	2.65	83.0	0.97	2.60	79.4
80	1 284	0.93	2.80	2.80	7 159.0	0.93	1.68	537.8	0.93	1.75	84.2	0.93	1.71	81.2

*All reported computational times are in milliseconds

The results indicate that the improved SOM v2 [31] and the herein proposed GSOA are far the fastest solvers for the OP. However, the traditional CGW heuristic [52] provides the best results. On the other hand, the 4-phase heuristic [51] provides in some cases worse solution than the unsupervised learning based approaches and overall both SOM and GSOA approaches can be considered competitive. Regarding the comparison of the proposed GSOA to the previous SOM-based approaches, the overall solution quality is competitive with the SOM v2. Based on the statistical evaluation of the average sum of the collected rewards among the performed trials using the t-test with the significance level of 0.05, the SOM v2 provides statistically significant better solutions for the Set 66 with $T_{max} \in \{60, 120\}$ and the GSOA provides better results for the Set 66 with $T_{max} \in \{45, 85\}$, which are highlighted in Table 2. In all other cases, differences in the solutions quality for both approaches (the SOM v2 and the herein proposed GSOA) are not statistically significant. However, the main expectations are in solutions of the Close Enough OP (CEOP) for which the results are reported in the following section.

5.3. GSOA in the Close Enough Orienteering Problem

The performance of the GSOA in the CEOP has been evaluated in the same problems as the comparison of the SOM v1 and SOM v2 reported in [31], i.e., in the Set 64 with $T_{max} = 45$ and Set 66 with $T_{max} = 60$, and $\delta \in \{0.0, 0.5, 1.0, 1.5, 2.0\}$. Besides, the newly introduced Set 130 with $T_{max} = 200$ and $T_{max} = 300$ and $\delta \in \{0, 1, 2, 3, 4\}$ is considered to show the performance of the CEOP solvers in larger instances. The average values of the solution cost R computed as the sum of the collected rewards are presented in Fig. 12a, Fig. 12b, and Fig. 13.

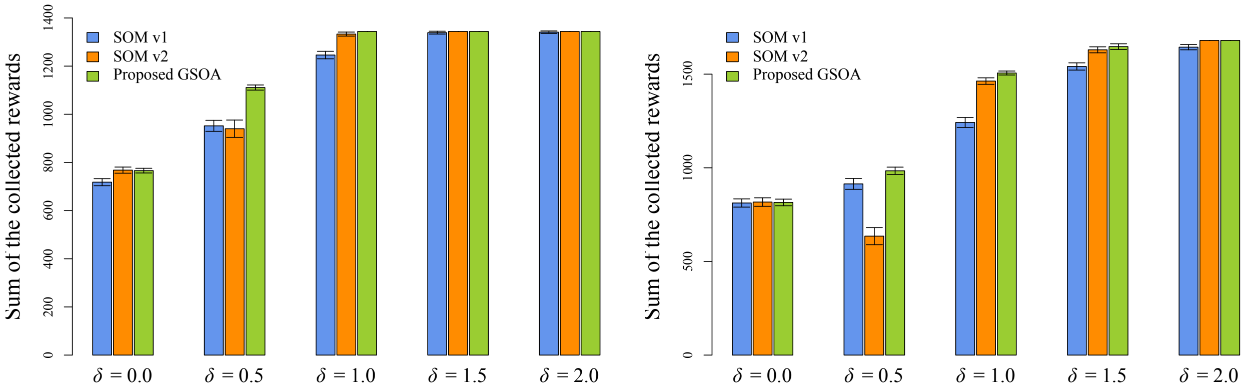

(a) Set 64, $T_{max} = 45$ (b) Set 66, $T_{max} = 60$

Figure 12: The average sums of the collected rewards in the OP Set 64 and Set 66 scenarios for the selected T_{max} and the communication range δ. The previous SOM-based approaches are denoted SOM v1 [30] and SOM v2 [31].

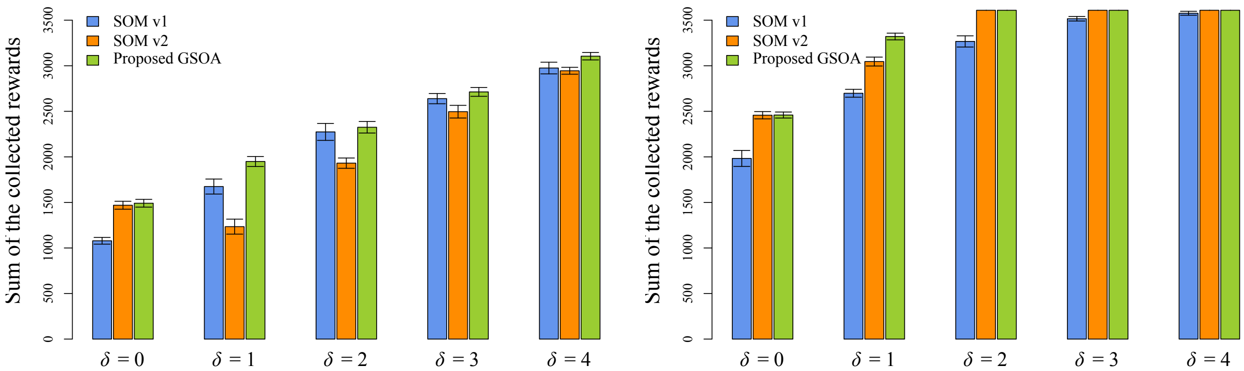

(a) Set 130, $T_{max} = 200$ (b) Set 130, $T_{max} = 300$

Figure 13: The average sums of the collected rewards in the OP Set 130 scenarios with the travel budget $T_{max} \in \{200, 300\}$ and the communication range δ. The previous SOM-based approaches are denoted SOM v1 [30] and SOM v2 [31].

Table 2: Performance of the Proposed GSOA solver for the OP in Set 66

T_{max}	R_{opt}	CGW	4-phase [51]			SOM v1 [30]			SOM v2 [31]			**Proposed GSOA**		
		RPE	RPE	ARPE	T_{CPU}*	RPE	ARPE	T_{CPU}*	RPE	ARPE	T_{CPU}*	RPE	ARPE	T_{CPU}*
15	120	0.00	25.00	25.00	122.0	0.00	0.00	281.4	0.00	0.00	15.0	0.00	0.00	15.4
20	205	4.88	0.00	0.00	517.0	0.00	1.46	561.6	0.00	3.90	22.8	0.00	2.80	22.2
25	290	0.00	6.90	6.90	1 298.0	0.00	2.16	864.0	0.00	3.45	26.1	0.00	3.19	25.4
30	400	0.00	7.50	7.50	1 383.0	0.00	9.88	1 001.3	3.75	8.88	29.9	0.00	8.50	28.0
35	465	1.08	0.00	0.00	1 151.0	2.15	7.58	1 134.0	5.38	8.01	32.0	3.23	6.61	31.8
40	575	0.00	6.96	6.96	1 115.0	6.96	12.48	1 252.0	6.09	11.96	36.8	6.96	10.52	34.8
45	650	0.00	5.38	5.38	2 099.0	0.77	10.81	1 330.0	6.15	11.58	39.8	1.54	9.31	39.1
50	730	0.00	0.00	0.00	2 256.0	4.11	10.99	1 394.4	4.79	10.45	44.8	6.85	9.69	45.0
55	825	0.00	1.21	1.21	2 422.0	5.45	11.30	1 395.2	3.03	10.48	49.3	4.24	9.76	46.2
60	915	0.00	2.19	2.19	2 405.0	7.65	11.56	1 407.2	7.65	10.38	54.2	9.29	11.53	50.6
65	980	0.00	0.00	0.00	2 295.0	1.02	9.69	1 422.6	4.59	7.88	59.2	3.57	7.76	56.3
70	1 070	0.00	0.93	0.93	2 148.0	5.14	9.49	1 413.4	2.80	7.20	63.7	2.34	7.55	60.1
75	1 140	0.00	2.63	2.63	3 252.0	5.26	9.50	1 409.0	2.63	6.58	67.2	4.39	6.64	63.4
80	1 215	0.00	3.29	3.29	3 418.0	6.17	9.09	1 379.4	4.12	6.13	70.1	2.88	6.03	67.7
85	1 270	0.00	3.15	3.15	3 057.0	3.94	7.97	1 346.4	3.54	5.22	72.8	1.97	4.45	71.2
90	1 340	0.00	0.75	0.75	4 382.0	5.22	8.04	1 305.7	2.24	4.44	75.9	2.61	4.40	74.4
95	1 395	1.08	0.00	0.00	4 240.0	4.66	6.67	1 250.6	2.87	4.44	79.6	3.23	4.07	78.3
100	1 465	2.05	0.00	0.00	5 488.0	3.41	6.55	1 194.8	2.05	4.71	80.6	2.73	4.25	79.8
105	1 520	0.66	0.00	0.00	5 030.0	3.29	5.81	1 121.1	3.29	4.67	82.6	2.30	4.01	81.8
110	1 560	0.64	0.64	0.64	6 370.0	2.56	4.65	1 063.4	2.24	3.53	85.0	1.92	3.48	81.8
115	1 595	0.00	0.00	0.00	7 501.0	0.94	2.54	986.6	0.94	2.40	85.8	0.94	2.08	85.5
120	1 635	0.00	0.00	0.00	8 362.0	0.00	1.15	909.3	0.00	1.15	87.2	0.92	1.61	84.9
125	1 670	0.90	0.00	0.00	9 262.0	0.00	1.12	713.3	0.60	1.09	88.8	0.90	1.05	88.4
130	1 680	0.00	0.00	0.00	10 030.0	0.00	0.36	496.7	0.00	0.12	67.8	0.00	0.12	88.9

*All reported computational times are in milliseconds

Overall, the proposed GSOA provides the best solutions and noticeably improves the performance of unsupervised learning based solution of the CEOP. It seems it solves the worse performance of the SOM v2 than SOM v1 in the Set 66 with $\delta = 0.5$, and it provides stable performance with the expected increase of the collected rewards with increasing the communication range δ. The computational requirements are similar to the SOM v2 as in the solution of the OP, and therefore, a presentation of detail results is omitted.

5.4. GSOA in the CEOP with Spatial Correlation

The proposed GSOA is the first solution of the CEOP with spatial correlations, and therefore, the performance of the solver is studied for all the travel budgets of the problems Set 64, Set 66, and Set 130. For the instances of the Set 64 and Set 66, the spatial correlations are modeled for the rewards radius $\xi = 0.5$, which can be compared with the mutual distance of the sensor locations in Fig. 9 where the communication range $\delta = 0.5$ is visualized.

Table 3: Performance of the Proposed GSOA solver for the OP in Set 130

T_{max}	R_{ref}	4-phase [51]			SOM v1 [30]			SOM v2 [31]			**Proposed GSOA**		
		RPE	ARPE	T_{CPU}*	RPE	ARPE	T_{CPU}*	RPE	ARPE	T_{CPU}*	RPE	ARPE	T_{CPU}*
50	375	0.80	0.80	781.0	0.00	5.08	1 620.5	0.00	0.73	22.3	0.00	0.28	26.8
100	816	42.56	42.56	15 935.0	22.68	30.08	3 284.7	0.98	4.98	65.2	0.00	3.80	66.3
150	1 238	14.97	14.97	17 356.0	28.88	36.98	3 403.2	3.80	9.66	90.2	0.00	9.09	95.3
200	1 608	8.03	8.03	18 764.0	24.22	34.29	4 217.6	2.08	9.26	121.8	0.00	7.67	127.7
250	2 104	0.00	0.00	21 857.0	26.05	30.53	5 248.6	4.13	7.78	165.2	1.05	8.30	170.6
300	2 647	0.00	0.00	27 675.0	16.51	23.00	6 062.9	3.55	7.62	214.7	5.82	7.50	221.2
350	3 111	0.00	0.00	36 083.0	6.49	13.03	5 764.6	2.09	4.82	257.4	2.44	4.28	264.6
400	3 521	1.96	1.96	48 885.0	0.34	3.36	4 127.9	0.00	1.92	285.1	0.77	1.91	286.6
410	3 609	5.62	5.62	47 137.0	0.67	2.84	3 662.6	0.00	1.91	281.5	0.72	1.84	289.0

*All reported computational times are in milliseconds

The correlation radius χ is selected from the set $\chi \in \{0, 1, 2\}$ and the communication radius δ is one of the three possible values $\delta \in \{0.0, 0.5, 1.0\}$. For the instances of the Set 130, a longer reward radius $\xi = 2.5$ is considered because of the large scale problem. The correlation radius χ and the communication radius δ are selected from the set $\chi \in \{0, 1, 2\}$ and $\delta \in \{0, 1, 2\}$, respectively. Detail results are depicted in Table 4, Table 5, and Table 6, where it can be noticed the maximal rewards $R = 1344$, $R = 1680$, $R = 3609$ for the Set 64, Set 66, and Set 130 respectively, are achieved for lower budgets because of increasing communication radius δ as well as exploiting the spatial correlations for increasing correlation radius χ.

Overall results are depicted in Fig. 14a and Fig. 14b. Selected best found solutions are visualized in Fig. 17, Fig. 18, Fig. 19, Fig. 20, Fig. 21, and Fig. 22.

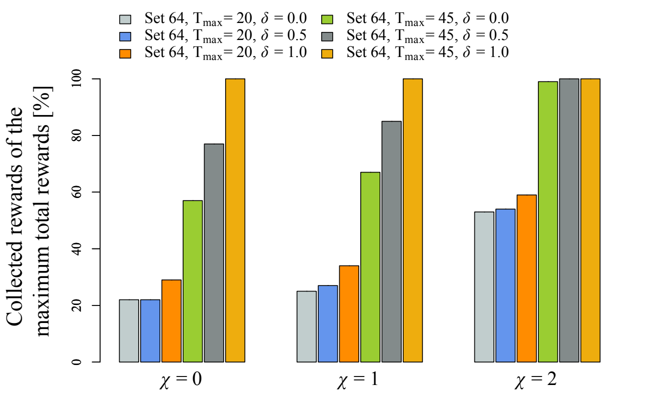

(a) Set 64 instances

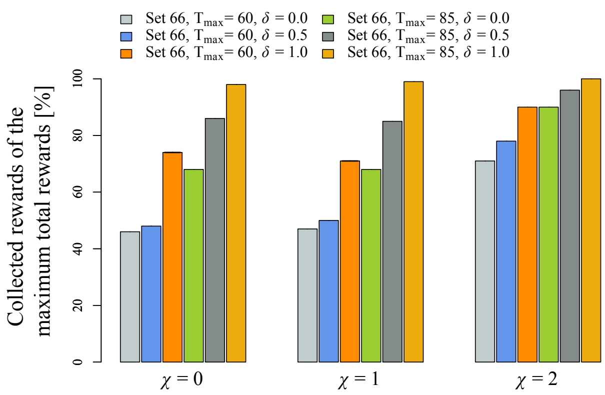

(b) Set 66 instances

Figure 14: The sums of the collected rewards in the OP instances of the Set 64 and Set 66 with the travel budget T_{max}, correlation radius χ, and communication range δ. The collected rewards are shown as the percentage of the total rewards in the scenario.

An overview of the solution improvement is shown in Fig. 14a for the Set 64 and selected $T_{max} = 20$ and $T_{max} = 45$. In Fig. 14b, the overview of the solution cost is presented for the Set 66 and $T_{max} = 60$ and $T_{max} = 85$. Both plots support the idea of improving the solution cost by considering not only non-zero communication radius δ but also the correlation radius χ.

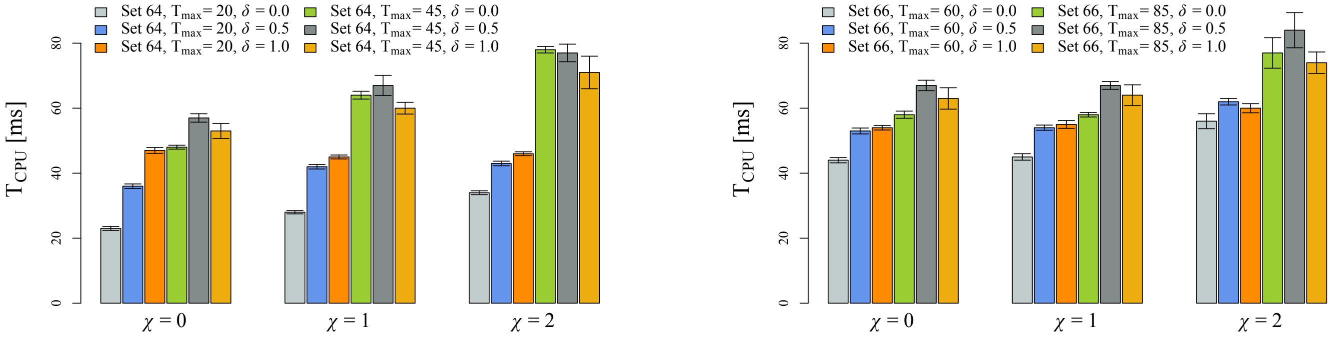

(a) Set 64 (b) Set 66

Figure 15: The average required computational times for solving the Set 64 and Set 66 instances of the CEOP with spatial correlations, the travel budget $\mathrm{T_{max}}$, correlation radius χ, and communication range δ.

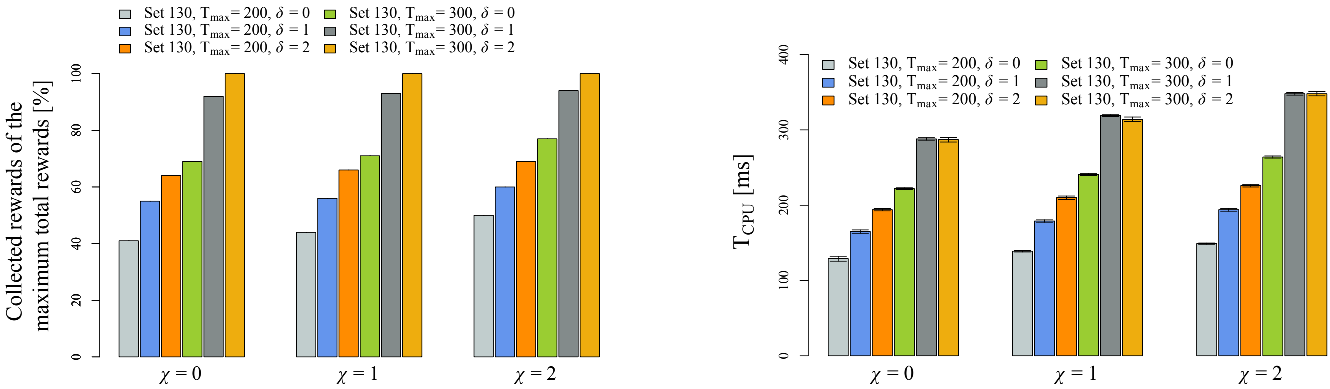

(a) Set 130, Collected rewards (b) Set 130, Computational requirements

Figure 16: The sum of the collected rewards and the average required computational times for the CEOP instances of the Set 130 with spatial correlations, the travel budget $\mathrm{T_{max}}$, correlation radius χ, and communication range δ.

An overview of the average required computational time is shown in Fig. 15. Again, the solution is provided in less than one hundred milliseconds, and increasing δ and χ makes the solution up to two times more demanding. Since the solution with the spatial correlations are found very quickly, the proposed approach can be directly employed in online decision-making as the early version of the SOM v1 [30], which is significantly slower than the proposed GSOA (e.g., see Table 4 and Table 5), in active perception [39], while it can save the computational power for demanding image processing or localization.

5.5. Discussion

Regarding the presented results, the proposed GSOA for the CEPCTSP and CEOP seems to be a vital alternative to the combinatorial approaches and also to the previous SOM-based unsupervised learning methods. Although the performance in solving the standard OP seems to be a bit worse than the previous SOM v2 [31], the GSOA provides statistically competitive results. Besides, the proposed GSOA provides better results in solving the CEOP. The most supportive results are presented for the CEOP with spatial correlations, where the solution can benefit in saving the travel cost by retrieving data within the δ communication range and avoiding data collection from sensors providing data with decreased information gain because of the collected data from the nearby sensors. The computational requirements of the GSOA are very low, and solutions are found in tens of milliseconds. Therefore a relatively high number of learning epochs $i_{max} = 500$ can be considered without a noticeable increase in the computational time. On the other hand, the current low computational requirements motivate for employing

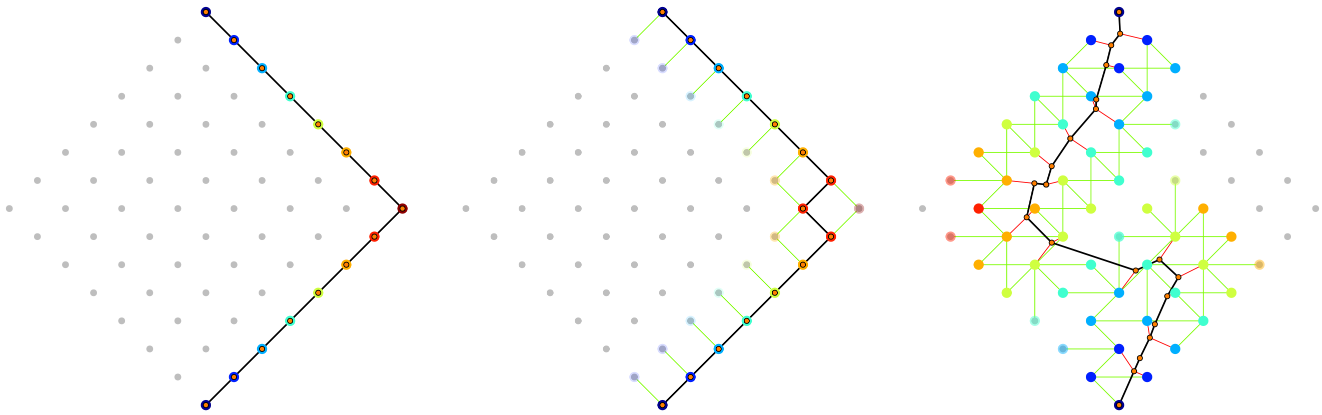

(a) $\mathrm{T_{max}} = 20$, $\delta = 0.0$, $\chi = 0$, $R = 294$ (b) $\mathrm{T_{max}} = 20$, $\delta = 0.0$, $\chi = 1$, $R = 340$ (c) $\mathrm{T_{max}} = 20$, $\delta = 1.0$, $\chi = 2$, $R = 927$

Figure 17: Selected best found solutions of the CEOP Set 64 scenarios with $\mathrm{T_{max}} = 20$, the communication radius δ, and correlation radius χ.

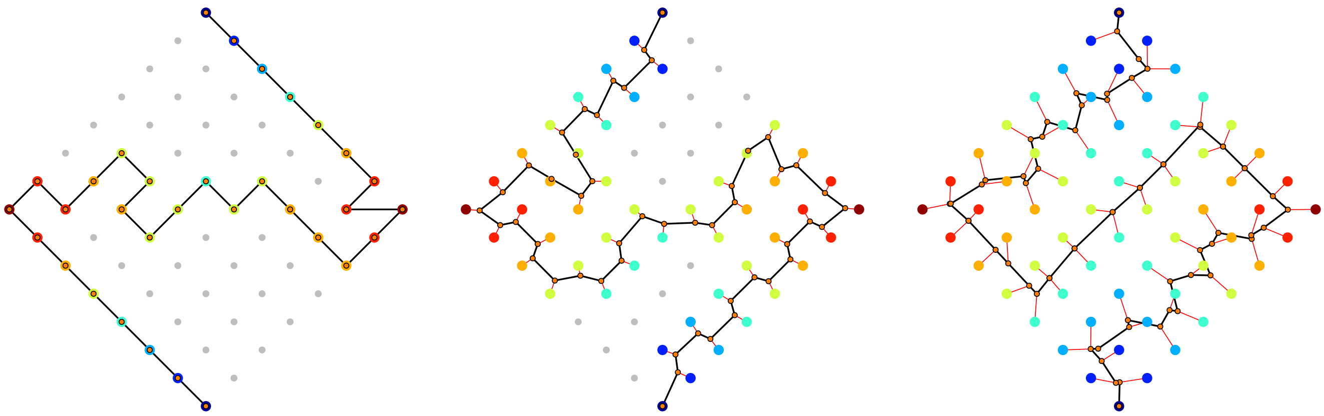

(a) $\mathrm{T_{max}} = 45$, $\delta = 0.0$, $\chi = 0$, $R = 792$ (b) $\mathrm{T_{max}} = 45$, $\delta = 0.5$, $\chi = 0$, $R = 1134$ (c) $\mathrm{T_{max}} = 45$, $\delta = 1.0$, $\chi = 0$, $R = 1344$

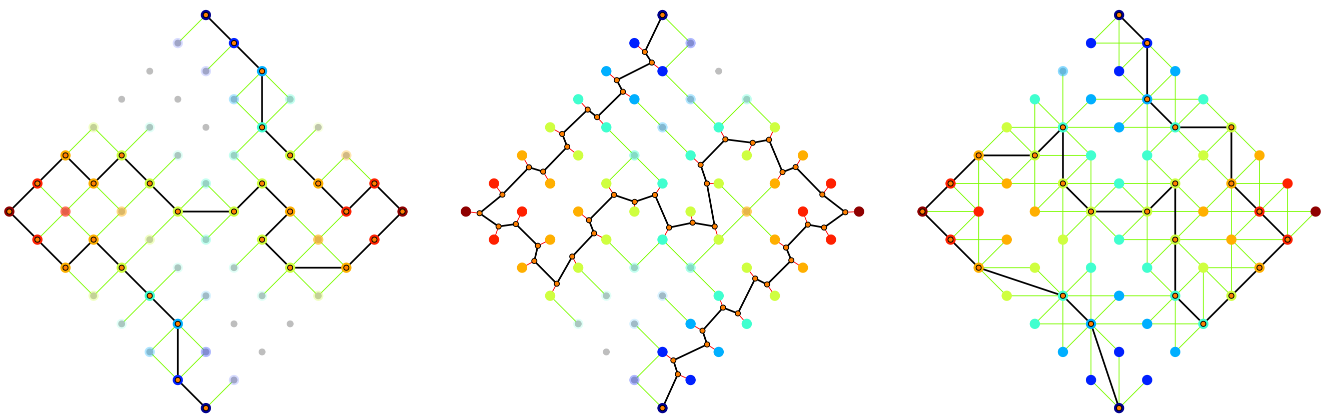

(d) $\mathrm{T_{max}} = 45$, $\delta = 0.0$, $\chi = 1$, $R = 913$ (e) $\mathrm{T_{max}} = 45$, $\delta = 0.5$, $\chi = 1$, $R = 1189$ (f) $\mathrm{T_{max}}$=45, $\delta = 0.0$, $\chi = 2$, $R = 1338$

Figure 18: Selected best found solutions of the CEOP Set 64 scenarios with $\mathrm{T_{max}} = 45$, the communication radius δ, and correlation radius χ.

other local optimization strategies, e.g., such as VNS [58], to improve the solution, especially in the solution of the standard OP.

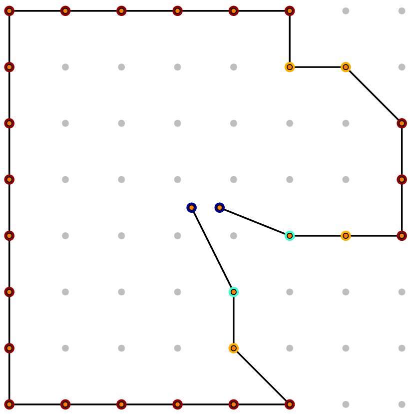

(a) $\mathrm{T_{max}} = 60$, $\delta = 0.0$, $\chi = 0$, $R = 865$

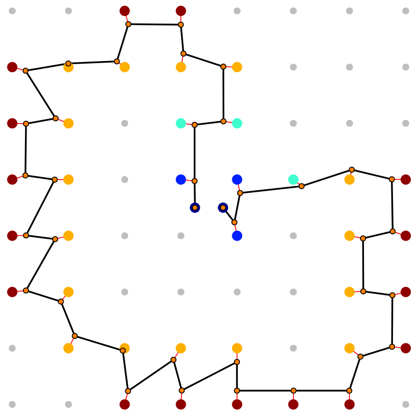

(b) $\mathrm{T_{max}} = 60$, $\delta = 0.5$, $\chi = 0$, $R = 1020$

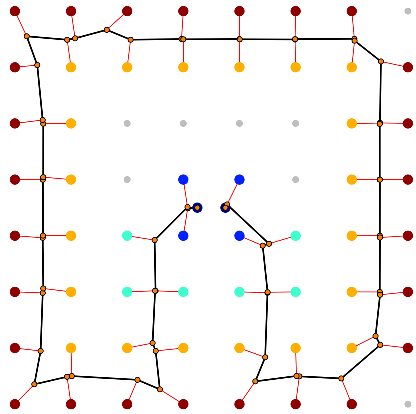

(c) $\mathrm{T_{max}} = 60$, $\delta = 1.0$, $\chi = 0$, $R = 1520$

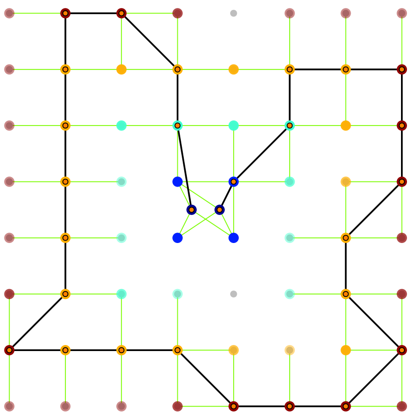

(d) $\mathrm{T_{max}} = 60$, $\delta = 0.0$, $\chi = 2$, $R = 1277$

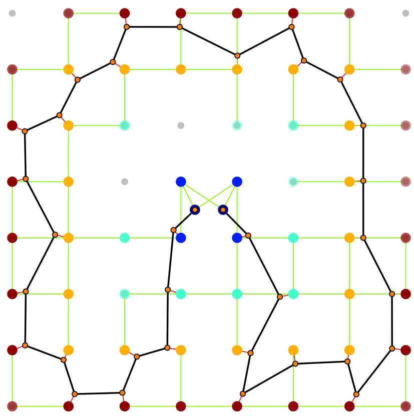

(e) $\mathrm{T_{max}} = 60$, $\delta = 0.5$, $\chi = 2$, $R = 1423$

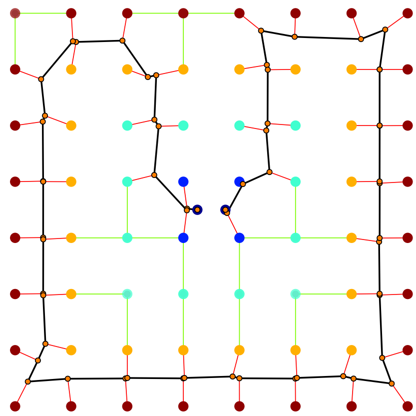

(f) $\mathrm{T_{max}} = 60$, $\delta = 1.0$, $\chi = 2$, $R = 1656$

Figure 19: Selected best found solutions of the CEOP Set 66 scenarios with $\mathrm{T_{max}} = 60$, the communication radius δ, and correlation radius χ.

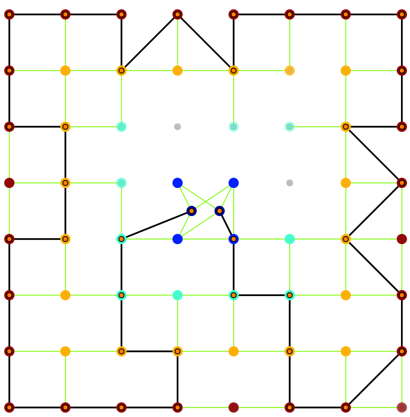

(a) $\mathrm{T_{max}} = 85$, $\delta = 0.0$, $\chi = 2$, $R = 1593$

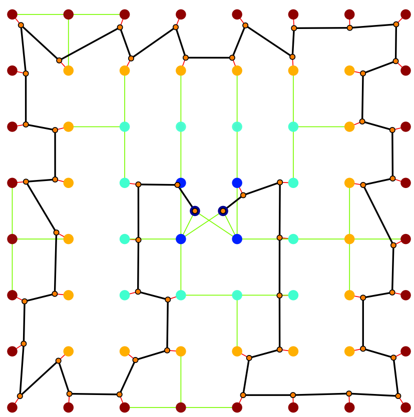

(b) $\mathrm{T_{max}} = 85$, $\delta = 0.5$, $\chi = 2$, $R = 1672$

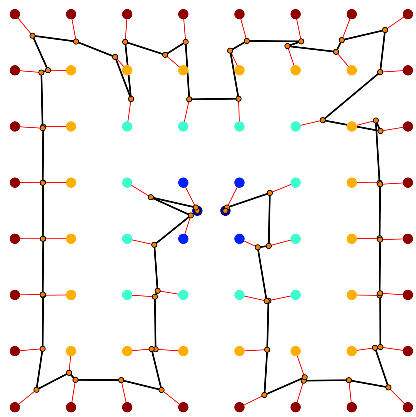

(c) $\mathrm{T_{max}} = 85$, $\delta = 1.0$, $\chi = 0$, $R = 1680$

Figure 20: Selected best found solutions of the CEOP Set 66 scenarios with $\mathrm{T_{max}} = 85$, the communication radius δ, and correlation radius χ.

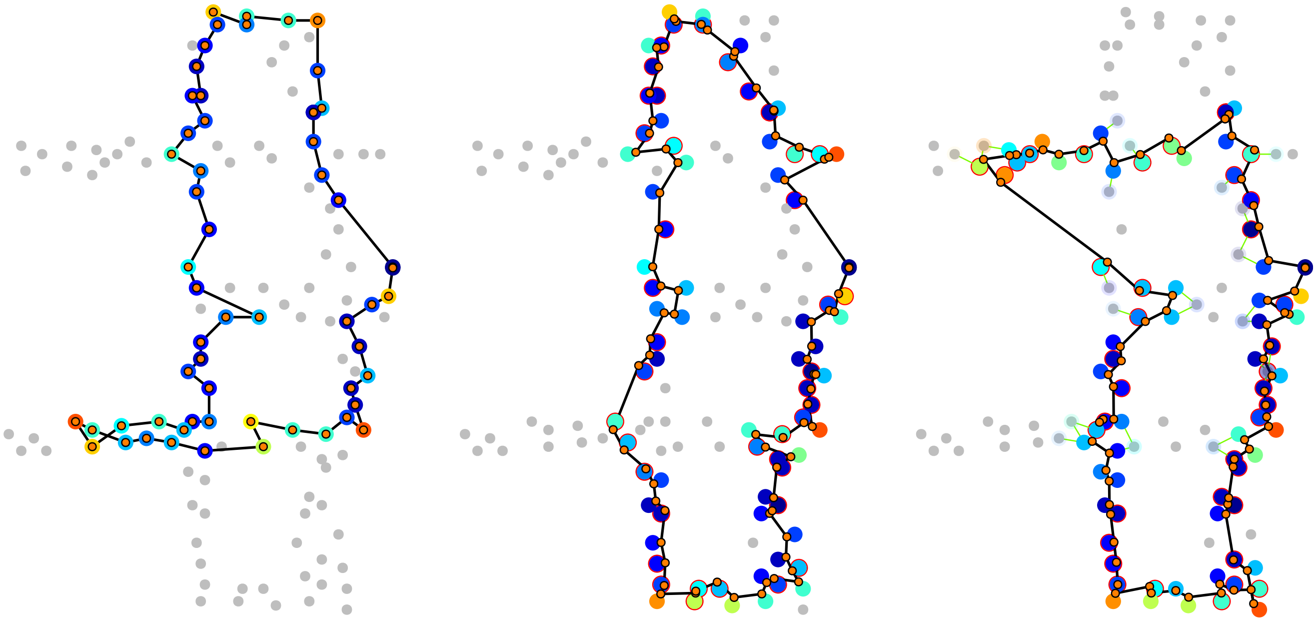

(a) $\mathrm{T_{max}} = 200$, $\delta = 0$, $\chi = 0$, $R = 1545$ (b) $\mathrm{T_{max}} = 200$, $\delta = 1$, $\chi = 0$, $R = 2113$ (c) $\mathrm{T_{max}} = 200$, $\delta = 1$, $\chi = 1$, $R = 2110$

Figure 21: Selected best found solutions of the CEOP Set 130 scenarios with $\mathrm{T_{max}} = 200$, the communication radius δ, and correlation radius χ. The initial and terminal locations are very close and they are the right most locations, approximately in the middle of the locations (vertically).

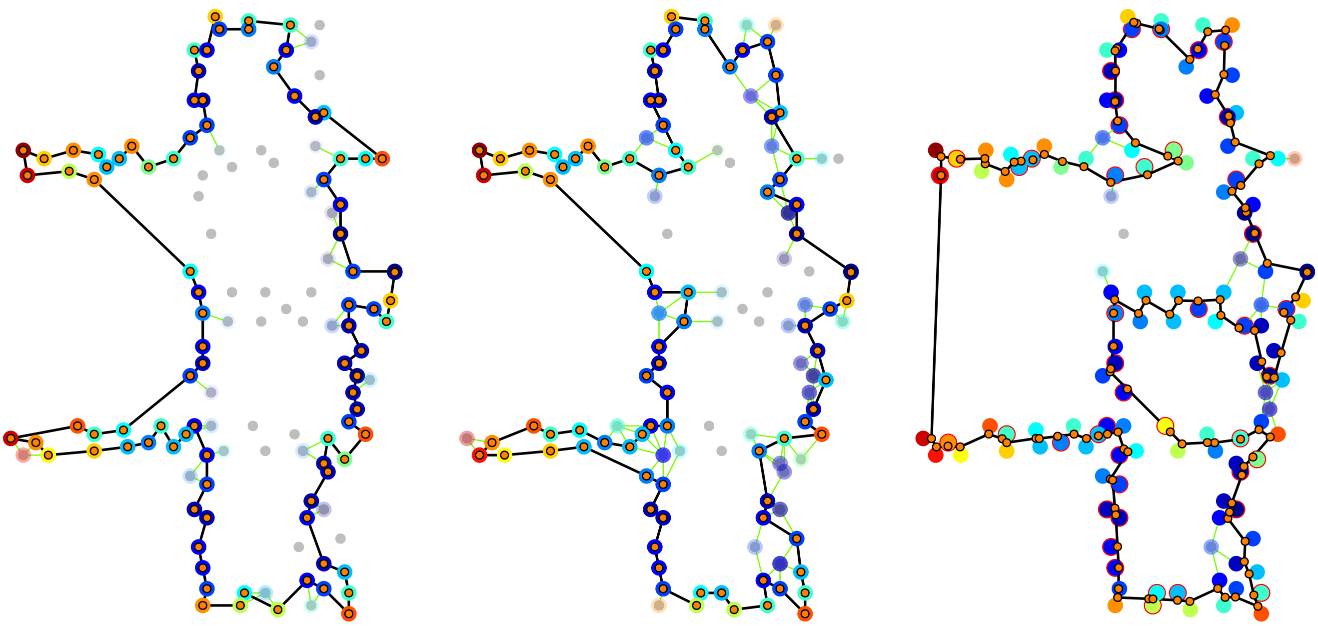

(a) $\mathrm{T_{max}} = 300$, $\delta = 0$, $\chi = 1$, $R = 2659$ (b) $\mathrm{T_{max}} = 300$, $\delta = 0$, $\chi = 2$, $R = 2835$ (c) $\mathrm{T_{max}} = 300$, $\delta = 1$, $\chi = 2$, $R = 3452$

Figure 22: Selected best found solutions of the CEOP Set 130 scenarios with $\mathrm{T_{max}} = 300$, the communication radius δ, and correlation radius χ.

Table 4: Performance of the proposed GSOA in the CEOP with spatially correlated measurements in the Set 64 problems

Problem, T_{max}	R for $\chi = 0$			R for $\chi = 1$			R for $\chi = 2$		
	$\delta = 0.0$	$\delta = 0.5$	$\delta = 1.0$	$\delta = 0.0$	$\delta = 0.5$	$\delta = 1.0$	$\delta = 0.0$	$\delta = 0.5$	$\delta = 1.0$
Set 64, $T_{max} = 15$	96	180	288	155	249	356	423	516	641
Set 64, $T_{max} = 20$	294	366	522	340	438	571	725	813	927
Set 64, $T_{max} = 25$	384	522	672	448	572	745	939	1068	1201
Set 64, $T_{max} = 30$	450	660	912	558	744	993	1180	1253	1325
Set 64, $T_{max} = 35$	570	834	1116	681	938	1174	1275	1313	1344
Set 64, $T_{max} = 40$	684	1026	1266	816	1091	1292	1318	1344	1344
Set 64, $T_{max} = 45$	792	1134	1344	913	1189	1344	1338	1344	1344
Set 64, $T_{max} = 50$	864	1212	1344	982	1271	1344	1343	1344	1344
Set 64, $T_{max} = 55$	960	1308	1344	1059	1315	1344	1344	1344	1344
Set 64, $T_{max} = 60$	1032	1344	1344	1117	1344	1344	1344	1344	1344
Set 64, $T_{max} = 65$	1086	1344	1344	1171	1344	1344	1344	1344	1344
Set 64, $T_{max} = 70$	1164	1344	1344	1234	1344	1344	1344	1344	1344
Set 64, $T_{max} = 75$	1224	1344	1344	1268	1344	1344	1344	1344	1344
Set 64, $T_{max} = 80$	1272	1344	1344	1300	1344	1344	1344	1344	1344

Table 5: Performance of the proposed GSOA in the CEOP with spatially correlated measurements in the Set 66 problems

Problem, T_{max}	R for $\chi = 0$			R for $\chi = 1$			R for $\chi = 2$		
	$\delta = 0.0$	$\delta = 0.5$	$\delta = 1.0$	$\delta = 0.0$	$\delta = 0.5$	$\delta = 1.0$	$\delta = 0.0$	$\delta = 0.5$	$\delta = 1.0$
Set 66, $T_{max} = 5$	10	20	20	14	20	20	48	75	75
Set 66, $T_{max} = 10$	40	70	95	44	74	95	113	158	210
Set 66, $T_{max} = 15$	120	160	200	125	164	207	240	295	362
Set 66, $T_{max} = 20$	205	255	345	210	257	327	381	429	529
Set 66, $T_{max} = 25$	290	365	500	297	360	465	489	556	679
Set 66, $T_{max} = 30$	400	450	605	390	439	579	606	709	821
Set 66, $T_{max} = 35$	455	520	760	455	529	732	725	807	920
Set 66, $T_{max} = 40$	545	650	860	545	644	844	835	938	1114
Set 66, $T_{max} = 45$	625	690	1025	640	745	1007	954	1083	1269
Set 66, $T_{max} = 50$	680	810	1180	720	815	1240	1072	1192	1405
Set 66, $T_{max} = 55$	765	910	1350	782	919	1345	1150	1320	1587
Set 66, $T_{max} = 60$	865	1020	1520	847	1020	1520	1277	1423	1656
Set 66, $T_{max} = 65$	940	1155	1620	945	1154	1620	1386	1528	1676
Set 66, $T_{max} = 70$	1020	1265	1665	1034	1274	1665	1438	1598	1680
Set 66, $T_{max} = 75$	1100	1390	1680	1097	1419	1680	1521	1639	1680
Set 66, $T_{max} = 80$	1175	1510	1680	1179	1519	1680	1553	1660	1680
Set 66, $T_{max} = 85$	1230	1580	1680	1239	1587	1680	1593	1672	1680
Set 66, $T_{max} = 90$	1310	1630	1680	1314	1629	1680	1625	1680	1680
Set 66, $T_{max} = 95$	1370	1670	1680	1385	1677	1680	1643	1680	1680
Set 66, $T_{max} = 100$	1420	1680	1680	1450	1680	1680	1659	1680	1680
Set 66, $T_{max} = 105$	1475	1680	1680	1484	1680	1680	1671	1680	1680
Set 66, $T_{max} = 110$	1540	1680	1680	1554	1680	1680	1676	1680	1680
Set 66, $T_{max} = 115$	1590	1680	1680	1589	1680	1680	1679	1680	1680
Set 66, $T_{max} = 120$	1625	1680	1680	1629	1680	1680	1680	1680	1680
Set 66, $T_{max} = 125$	1670	1680	1680	1670	1680	1680	1680	1680	1680
Set 66, $T_{max} = 130$	1680	1680	1680	1680	1680	1680	1680	1680	1680

Table 6: Performance of the proposed GSOA in the CEOP with spatially correlated measurements in the Set 130 problems

Problem, T_{max}	R for $\chi = 0$			R for $\chi = 1$			R for $\chi = 2$		
	$\delta = 0$	$\delta = 1$	$\delta = 2$	$\delta = 0$	$\delta = 1$	$\delta = 2$	$\delta = 0$	$\delta = 1$	$\delta = 2$
Set 130, $T_{max} = 50$	375	462	530	390	473	534	420	501	574
Set 130, $T_{max} = 100$	839	1092	1254	857	1135	1291	1010	1184	1333
Set 130, $T_{max} = 150$	1185	1527	1769	1267	1568	1808	1407	1702	1885
Set 130, $T_{max} = 200$	1545	2113	2408	1671	2110	2507	1871	2322	2625
Set 130, $T_{max} = 250$	2042	2776	3207	2197	2828	3249	2343	2895	3301
Set 130, $T_{max} = 300$	2555	3389	3609	2659	3417	3609	2835	3452	3609
Set 130, $T_{max} = 350$	3036	3609	3609	3089	3609	3609	3233	3609	3609
Set 130, $T_{max} = 400$	3503	3609	3609	3509	3609	3609	3549	3609	3609
Set 130, $T_{max} = 410$	3584	3609	3609	3593	3609	3609	3599	3609	3609

6. Conclusion

The herein proposed GSOA-based solution for solving the Close Enough Prize-Collecting Traveling Salesman Problem and Close Enough Orienteering Problem (both with spatial correlations) represents a unifying approach for data collection planning where it is requested to determine a cost-efficient path to retrieve the most rewarding sensor measurements from a set of pre-deployed sensors. The proposed solution allows exploiting not only the remote reading of the data from the sensors but also possible spatial correlations where data from one sensor includes information about the measurements from nearby locations. The proposed GSOA solver has low computational requirements and based on the previous comparison of the SOM-based solvers with combinatorial heuristics in the solution of the PCTSP. It provides better results. Moreover, the GSOA improves performance in a solution of the CEOP that is a suitable formulation of the data collection missions with the limited travel budget, which better fits the limitations of real robotic platforms. The reported results support the feasibility of the proposed approach and the current computational requirements of the GSOA technique provides a groundwork for further improvements of the solution quality or generalization for data collection planning for a team of vehicles.

On the other hand, the utilized distant based spatial correlations model is a general model that is easy to compute, and a more complex relation of the spatiotemporal field can be more demanding. Therefore, one of the planned future work is to employ the proposed GSOA in mission scenarios with a more complex model of the spatiotemporal field, where the studied phenomena are not static, and the rewards vary in time.

Acknowledgement

The presented work has been supported by the Czech Science Foundation (GAČR) under research project 15-09600Y. The author acknowledges the support of the OP VVV funded project CZ.02.1.01/0.0/0.0/16_019/0000765 "Research Center for Informatics".

7. References

[1] D. Bhadauria, O. Tekdas, V. Isler, Robotic data mules for collecting data over sparse sensor fields, Journal of Field Robotics 28 (3) (2011) 388–404.

[2] R. Smith, M. Schwager, S. Smith, B. H. Jones, D. Rus, G. Sukhatme, Persistent ocean monitoring with underwater gliders: Adapting sampling resolution, Journal of Field Robotics 28 (5) (2011) 714–741.

[3] M. D. Kohler, P. J. Lynett, M. R. Legg, D. S. Weeraratne, Importance of large-scale bathymetry features on 2011 Tohoku tsunami waveforms through comparison of simulations with the spatially dense ALBACORE OBS array data, American Geophysical Union (AGU) Fall Meeting Abstracts (2012) S51B–2419.

[4] R. N. Smith, J. Das, H. K. Heidarsson, A. A. Pereira, F. Arrichiello, I. Cetinic, L. Darjany, M.-E. Garneau, M.-D. Howard, C. Oberg, M. Ragan, E. Seubert, E. C. Smith, B. Stauffer, A. Schnetzer, G. Toro-Farmer, D. A. Caron, B. H. Jones, G. S. Sukhatme, USC CINAPS builds bridges: Observing and monitoring the Southern California Bight, IEEE Robotics Automation Magazine 17 (1) (2010) 20–30.

[5] S. L. Nooner, W. W. Chadwick Jr., Volcanic inflation measured in the caldera of axial seamount: Implications for magma supply and future eruptions, Geochemistry, Geophysics, Geosystems 10 (2).

[6] G. Astuti, G. Giudice, D. Longo, C. D. Melita, G. Muscato, A. Orlando, An Overview of the “Volcan Project”: An UAS for Exploration of Volcanic Environments, Journal of Intelligent and Robotic Systems 54 (1-3) (2009) 471–494.

[7] M. Trincavelli, M. Reggente, S. Coradeschi, A. Loutfi, H. Ishida, A. J. Lilienthal, Towards environmental monitoring with mobile robots, in: IEEE/RSJ International Conference on Intelligent Robots and Systems (IROS), 2008, pp. 2210–2215.

[8] M. Bryson, A. Reid, F. Ramos, S. Sukkarieh, Airborne vision-based mapping and classification of large farmland environments, Journal Field Robotics 27 (5) (2010) 632–655.

[9] M. Dunbabin, L. Marques, Robots for Environmental Monitoring: Significant Advancements and Applications, IEEE Robotics Automation Magazine 19 (1) (2012) 24–39.

[10] D. Applegate, R. Bixby, V. Chvátal, W. Cook, The Traveling Salesman Problem: A Computational Study, Princeton University Press, Princeton, NJ, USA, 2007.

[11] G. Hollinger, S. Choudhary, P. Qarabaqi, C. Murphy, U. Mitra, G. Sukhatme, M. Stojanovic, H. Singh, F. Hover, Underwater data collection using robotic sensor networks, IEEE Journal on Selected Areas in Communications 30 (5) (2012) 899–911.

[12] D. J. Gulczynski, J. W. Heath, C. C. Price, The Close Enough Traveling Salesman Problem: A Discussion of Several Heuristics, Springer US, Boston, MA, 2006, pp. 271–283.

[13] Bo Yuan, M. Orlowska, S. Sadiq, On the Optimal Robot Routing Problem in Wireless Sensor Networks, IEEE Transactions on Knowledge and Data Engineering 19 (9) (2007) 1252–1261.

[14] I. Gentilini, F. Margot, K. Shimada, The travelling salesman problem with neighbourhoods: MINLP solution, Optimization Methods and Software 28 (2) (2013) 364–378.

[15] J. Dong, N. Yang, M. Chen, Heuristic Approaches for a TSP Variant: The Automatic Meter Reading Shortest Tour Problem, Springer US, Boston, MA, 2007, pp. 145–163.

[16] W. K. Mennell, Heuristics for solving three routing problems: Close-enough traveling salesman problem, close-enough vehicle routing problem, sequence-dependent team orienteering problem, Ph.D. thesis, University of Maryland (2009).

[17] K. Vicencio, B. Davis, I. Gentilini, Multi-goal path planning based on the generalized traveling salesman problem with neighborhoods, in: IEEE/RSJ International Conference on Intelligent Robots and Systems (IROS), 2014, pp. 2985–2990.

[18] J. Faigl, V. Vonásek, L. Přeučil, Visiting Convex Regions in a Polygonal Map, Robotics and Autonomous Systems 61 (10) (2013) 1070–1083.

[19] J. Faigl, GSOA: Growing self-organizing array – unsupervised learning for the close-enough traveling salesman problem and other routing problems, Neurocomputing 312 (2018) 120–134. doi:10.1016/j.neucom.2018.05.079.

[20] G. Laporte, A. Asef-Vaziri, C. Sriskandarajah, Some applications of the generalized travelling salesman problem, Journal of the Operational Research Society 47 (12) (1996) 1461–1467.

[21] K. Helsgaun, Solving the equality generalized traveling salesman problem using the lin–kernighan–helsgaun algorithm, Mathematical Programming Computation 7 (3) (2015) 269–287.

[22] S. L. Smith, F. Imeson, GLNS: An effective large neighborhood search heuristic for the generalized traveling salesman problem, Computers & Operations Research 87 (2017) 1–19.

[23] F. Carrabs, C. Cerrone, R. Cerulli, M. Gaudioso, A novel discretization scheme for the close enough traveling salesman problem, Computers & Operations Research 78 (2017) 163–171.

[24] J. Goerner, N. Chakraborty, K. Sycara, Energy efficient data collection with mobile robots in heterogeneous sensor networks, in: IEEE International Conference on Robotics and Automation (ICRA), 2013, pp. 2527–2533.

[25] E. Balas, The prize collecting traveling salesman problems, Networks 19 (1989) 621–636.

[26] G. Hollinger, U. Mitra, G. Sukhatme, Autonomous data collection from underwater sensor networks using acoustic communication, in: IEEE/RSJ International Conference on Intelligent Robots and Systems (IROS), 2011, pp. 3564–3570.

[27] B. L. Golden, L. Levy, R. Vohra, The orienteering problem, Naval Research Logistics (NRL) 34 (3) (1987) 307–318.

[28] A. Gunawan, H. C. Lau, P. Vansteenwegen, Orienteering Problem: A survey of recent variants, solution approaches and applications, European Journal of Operational Research 255 (2) (2016) 315–332.

[29] G. Best, J. Faigl, R. Fitch, Multi-robot path planning for budgeted active perception with self-organising maps, in: IEEE/RSJ International Conference on Intelligent Robots and Systems (IROS), 2016, pp. 3164–3171.

[30] J. Faigl, R. Pěnička, G. Best, Self-organizing map-based solution for the orienteering problem with neighborhoods, in: IEEE International Conference on Systems, Man, and Cybernetics (SMC), 2016, pp. 1315–1321.

[31] J. Faigl, On self-organizing maps for orienteering problems, in: International Joint Conference on Neural Networks (IJCNN), 2017, pp. 2611–2620.

[32] K.-C. Ma, L. Liu, G. S. Sukhatme, An information-driven and disturbance-aware planning method for long-term ocean monitoring, in: IEEE/RSJ International Conference on Intelligent Robots and Systems (IROS), 2016, pp. 2102–2108.

[33] J. Faigl, G. A. Hollinger, Autonomous data collection using a self-organizing map, IEEE Transactions on Neural Networks and Learning Systems 29 (5) (2018) 1703–1715.

[34] J. Faigl, P. Váňa, Self-organizing map for data collection planning in persistent monitoring with spatial correlations, in: IEEE International Conference on Systems, Man, and Cybernetics (SMC), 2016, pp. 3264–3269.

[35] M. Goemans, D. P. Williamson, A general approximation technique for constrained forest problems, SIAM Journal on Computing 24 (2) (1995) 296–317.

[36] A. Archer, M. H. Bateni, H. M. T., H. Karloff, Improved approximation algorithms for prize-collecting steiner tree and tsp, SIAM Journal on Computing 40 (2) (2011) 309–332.

[37] J. Faigl, G. Hollinger, Self-organizing map for the prize-collecting traveling salesman problem, in: Advances in Self-Organizing Maps and Learning Vector Quantization: Proceedings of the 10th International Workshop (WSOM), 2014, pp. 281–291.

[38] P. Vansteenwegen, W. Souffriau, D. V. Oudheusden, The orienteering problem: A survey, European Journal of Operational Research 209 (1) (2011) 1–10.

[39] G. Best, J. Faigl, R. Fitch, Online planning for multi-robot active perception with self-organising maps, Autonomous Robots 42 (4) (2018) 715–736.

[40] R. Pěnička, J. Faigl, P. Váňa, M. Saska, Dubins orienteering problem with neighborhoods, in: International Conference on Unmanned Aircraft Systems (ICUAS), 2017, pp. 1555–1562.

[41] J. Yu, M. Schwager, D. Rus, Correlated Orienteering Problem and its Application to Persistent Monitoring Tasks, IEEE Transactions on Robotics 32 (5) (2016) 1106–1118.

[42] T. Yamakawa, K. Horio, M. Hoshino, Self-organizing map with input data represented as graph, in: Neural Information Processing, 2006, pp. 907–914.

[43] J. Faigl, On self-organizing map and rapidly-exploring random graph in multi-goal planning, in: Advances in Self-Organizing Maps and Learning Vector Quantization, 2016, pp. 143–153.

[44] J. Faigl, J. Mačák, Multi-goal path planning using self-organizing map with navigation functions, in: European Symposium on Artificial Neural Networks (ESANN), 2011, pp. 41–46.

[45] A.-J. Muñoz-Vázquez, V. Parra-Vega, A. Sánchez-Orta, F. Ruiz-Sánchez, A novel force-velocity field for object manipulation with a model-free cooperative controller, Transactions of the Institute of Measurement and Controldoi:10.1177/0142331218762272.

[46] E. M. Cochrane, J. E. Beasley, The co-adaptive neural network approach to the Euclidean travelling salesman problem, Neural Networks 16 (10) (2003) 1499–1525.

[47] J. Zhang, X. Feng, B. Zhou, D. Ren, An overall-regional competitive self-organizing map neural network for the euclidean traveling salesman problem, Neurocomputing 89 (2012) 1–11.

[48] J. Faigl, L. Přeučil, Inspection planning in the polygonal domain by self-organizing map, Applied Soft Computing 11 (8) (2011) 5028–5041.

[49] G. Reinelt, TSPLIB - A Traveling Salesman Problem Library, Journal on Computing 3 (4) (1991) 376–384.

[50] J. Faigl, On the performance of self-organizing maps for the non-euclidean traveling salesman problem in the polygonal domain, Information Sciences 181 (2011) 4214–4229.

[51] R. Ramesh, K. M. Brown, An efficient four-phase heuristic for the generalized orienteering problem, Computers & Operations Research 18 (2) (1991) 151–165.

[52] I.-M. Chao, B. L. Golden, E. A. Wasil, A fast and effective heuristic for the orienteering problem, European Journal of Operational Research 88 (3) (1996) 475–489.

[53] The Orienteering Problem: Test Instances – Department of Mechanical Engineering, citied on 2018-01-30. URL http://www.mech.kuleuven.be/en/cib/op#section-0

[54] J. Faigl, G. Hollinger, Unifying multi-goal path planning for autonomous data collection, in: IEEE/RSJ International Conference on Intelligent Robots and Systems (IROS), 2014, pp. 2937–2942.

[55] S. Muthuswamy, S. S. Lam, Discrete particle swarm optimization for the team orienteering problem, Memetic Computing 3 (4) (2011) 287–303.

[56] D.-C. Dang, R. N. Guibadj, A. Moukrim, An effective PSO-inspired algorithm for the team orienteering problem, European Journal of Operational Research 229 (2) (2013) 332–344.

[57] C. Archetti, A. Hertz, M. G. Speranza, Metaheuristics for the team orienteering problem, Journal of Heuristics 13 (1) (2007) 49–76.

[58] P. Hansen, N. Mladenović, Variable neighborhood search: Principles and applications, European Journal of Operational Research 130 (3) (2001) 449–467.